

# A MECHANICAL EXOSKELETON

by

Shaojun Ma

A Thesis

Presented to the Graduate and Research Committee of

Lehigh University

in Candidacy for the Degree of

Master of Science

in

Mechanical Engineering and Mechanics

Lehigh University

May, 2016

This thesis is accepted and approved in partial fulfillment of the requirements for the Master of Science.

---

Date

---

Thesis Advisor

---

Chairperson of Department

## **ACKNOWLEDGMENTS**

First, I would like to thank my advisor, Professor Meng-Sang Chew. Without his encouragement, instructions, and guidance during my study, I could not finish my thesis. In this two years, the most important thing Professor Meng-Sang Chew taught me is how to think as an engineer. Moreover, my advisor's humor, patience and kindness also help me know how to be a good researcher in the future.

Secondly, during my Master's study at Lehigh University, I deeply enjoyed my courses and thesis work. I have learned not only the knowledge, but also the purest attitude to study from faculty and staff. I will keep this deep in my mind to guide my future study and research.

Finally, I would like to express my deepest appreciation to my parents and friends for their endless support. I also want to thank my girlfriend for her company, she made every day of mine full of sunshine.

## Table of Contents

ACKNOWLEDGMENTS.....	iii
LIST OF FIGURES.....	v
ABSTRACT.....	1
<b>Chapter 1. Introduction.....</b>	<b>2</b>
1.1 Research Background of Exoskeleton and Suspension System.....	2
1.2 Introduction of Chapters Arrangement.....	11
<b>Chapter 2. Mechanism of 2-D Suspension System and Exoskeleton.....</b>	<b>12</b>
2.1 Mechanism of 2-D Suspension System.....	12
2.2 Mechanism of Exoskeleton System.....	15
<b>Chapter 3. 3-D Model of Exoskeleton.....</b>	<b>18</b>
3.1 Introduction of 3-D Model of Exoskeleton.....	18
3.2 Working Principle of 3-D Exoskeleton.....	22
<b>Chapter 4. Walking Assistive Systems in Exoskeleton.....</b>	<b>25</b>
4.1 Introduction of Clutch System.....	25
4.2 Introduction of Cable Release System.....	32
<b>Chapter 5. Two Dimensional Shape Optimization of Back Part in Exoskeleton..</b>	<b>41</b>
5.1 Introduction of Topology Optimization.....	41
5.2 Application of Topology Optimization in Exoskeleton.....	45
REFERENCE.....	51
APPENDIX.....	53
VITA.....	56

# LIST OF FIGURES

## Chapter 1. Introduction

Fig 1.1 (a) Happyback (b)Bendezy (c)BNDR.....	4
Fig 1.2 (a) HAL (b)HULC (c)BLEEX.....	7
Fig 1.3 (a) LEE (b)Moon-Walker (c)Soft Exosuit.....	9

## Chapter 2. Mechanism of 2-D Suspension System and Exoskeleton

Fig 2.1 Concept of the Two Degree-of-freedom Suspension System from Chi-Hung Cheng's Thesis in 2011.....	14
Fig 2.2 Concept of the exoskeleton system.....	17

## Chapter 3. 3-D Model of Exoskeleton

Fig 3.1 Basic 3-D model of exoskeleton in Solidworks.....	20
Fig 3.2 Basic 3-D model of exoskeleton in Solidworks (main components indicated).....	21
Fig 3.3 The exoskeleton at standing stage.....	23
Fig 3.4 The exoskeleton at crouching stage.....	24

## Chapter 4. Walking Assistive Systems in Exoskeleton

Fig 4.1 3-D model of clutch system at original stage.....	30
Fig 4.2 3-D model of clutch system at lock stage.....	31
Fig 4.3 3-D model of cable release system.....	36
Fig 4.4 Side view of cable release system.....	37
Fig 4.5 3-D model of walking assistive system.....	38
Fig 4.6 3-D model of whole exoskeleton system.....	39

Fig 4.7 walking assistive system in the whole exoskeleton system..... 40

**Chapter 5. Two Dimensional Shape Optimization of Back Part in Exoskeleton**

Fig 5.1 Two-dimensional model of back part exoskeleton..... 46

Fig 5.2 Results of simulation, the back part exoskeleton 2-D  
shapes under different volume rate requirements.....49

## **ABSTRACT**

### **A MECHANICAL EXOSKELEON**

Shaojun Ma

Lehigh University, 2016

Director: Dr. M. Chew

The purpose of this thesis is to design a 3-D exoskeleton model based on the mechanism of a kind of two degree-of-freedom suspension system. There are two main systems in the exoskeleton, including weight support system and walking assistive system. The weight support system consists a series of linkages, pulleys and springs, which is able to compensate wearer's weight, make wearer feel much more easier when keeps a crouching posture. The walking assistive system consists clutch system and cable release system, which is able to help exoskeleton walk when led by wearer.

In our exoskeleton design, excluding hydraulic and electric systems, we adopt pure mechanical systems, thus the whole system will be simple, light, clean, cheap and easy to build, the power provided by the exoskeleton will not be large. We also introduce the technique of exoskeleton shape optimization, which deserves more research in the future.

## **Chapter 1. Introduction**

### **1.1 Research Background of Exoskeleton and Suspension System**

The research of exoskeleton began in the late 1960s, almost in parallel between a number of research groups in the United States and in the former Yugoslavia. However, the former was primarily focused on developing technologies to augment the abilities of able-bodied humans, often for military purposes, while the latter was intent on developing assistive technologies for disabled people or whoever needs the help of the device. Usually, by activated method, the exoskeleton can be divided to positive, half-positive and passive.

Passive actuated exoskeleton means that the exoskeletons has no electrical, pneumatic or hydraulic actuators, elastic material like springs are widely used among them, through these springs, the devices are able to store and release power, help wearers use and save energy efficiently. These exoskeletons such as Happyback (ErgoAg Company, P.O. Box 1087, Aptos CA. 95001 n.d., Roberts and Bruce 1999), Bendezy (Mitchell and Timothy John 2002), BNDR (Deamer, Richard M. 1989, Anderson, Robert B. 1993), PLAD (Graham, Ryan B., Michael J. Agnew 2009) are able to reduce muscles fatigue when wearers are walking or crouching.

The Happyback is composed of fiberglass rods and fabric; it contains a chest harness, a low back pad, and thigh straps that wrap around and buckle together above the knees. The fiberglass rods have memory, and when bent they attempt to bring the user back to an upright position; this lift component allows the body to reach



equilibrium in a forward bent position, thus removing stress from the low back. The Bendezy is an all-metal support, with backpack-like straps as well as feet and ankle straps. Extending from a counterweight lever, springs load when the operator bends to lift the load and remove stresses from the spine and ES muscles. Lastly, the BNDR is a metal frame with a resistive articulation around the hip joint and pads at the thighs and chest; these resist forward bending and therefore take some of the load off the lumbar spine.

Without so much heavy, large actuators, and support mechanism, the advantages of passive exoskeleton are obvious. Firstly, the whole system is relatively light, so people can easily wear these devices. Secondly, the cost of passive exoskeleton is relatively cheaper. Thirdly, passive exoskeletons don't need outside power supply and complex control methods, thus they can work safely for a long time. The disadvantages are obvious too, without different actuators, outside power supply and support mechanism, passive exoskeletons are not able to help us hold too much weight.



(a)

(b)

(c)

Fig 1.1 (a) Happyback (b)Bendezy (c)BNDR

Positive actuated exoskeleton means that the exoskeleton is actuated purely by electrical, pneumatic or hydraulic actuators, without elastic materials. We can see several positive such as HAL (Sankai 2010), HULC (Berkeley Bionics & Lockheed-Martin 2009) and BLEEX (H. Kazerooni, et al. 2004).

The leg structure of HAL exoskeleton powers the flexion/extension joints at the hip and knee via DC motors with harmonic drive placed directly on the joints. The lower limb components interface with the wearer via several connections: a special shoe with ground reaction force sensors harnesses on the calf and thigh, and a large waist belt. For HULC, the wearer is able to walk at the average speed of 4.8 kilometers per hour while carrying 90 kilograms of load. BLEEX is actuated via hydraulic cylinders mounted in a triangular configuration with the rotary joints. According the experiments, BLEEX consumes an average of 1143 W of hydraulic power during level-ground walking, as well as 200 W of electrical power for the electronics and control. Users wearing BLEEX can reportedly support a load of up to 75 kg while walking at 0.9 m/s, and can walk at speeds of up to 1.3 m/s without the load.

These devices consist of hydraulic actuators, motors, batteries, thus the devices are all large, heavy and high stiffness when compared with passive devices, they are not economically feasible. With so much actuators, the control methods will be complex too, the systems also need a lot of power to work well, which will be very inconvenience. Moreover, if there is something wrong of the systems, it would be difficult to repair them because there are too much things we need to focus on due to the large volume of the system. However, despite these disadvantages, the positive

actuated exoskeletons are able to help people hold a very heavy weight, people can wear these devices to lift and move heavy things.



(a)



(b)



(c)

Fig 1.2 (a) HAL (b)HULC (c)BLEEX

Nowadays, researchers are paying much more attention on half-positive actuated exoskeletons. Half-positive means that in the exoskeletons, both positive actuators and elastic material are adopted, but positive actuators are relatively less than those in positive exoskeletons. This kind of exoskeleton system is relatively simple, but can help people do more work than pure passive exoskeleton. We can find this kind of exoskeleton such as a weight-support lower-extremity-exoskeleton (LEE)(Kok-Meng Lee & Donghai Wang), which is able to relieve compressive load in the knee via a compliant joint, meanwhile, this exoskeleton is able to help support wearer's weight by fabric and elastic materials. When wearing Moon-Walker(Sébastien Krut et al. 2010), wearer's body weight is compensated by using a passive force balancer, and a low power actuator is used for control, the strategy is loading the exoskeleton on the side where the user's leg is in stance, and lowering it on the side where the user's leg is in swing. A Lightweight Soft Exosuit presented by Michael Wehner et al. 2013, is able to augment the normal muscle work of healthy individuals by applying assistive torques at the wearer's hip and/or ankle during the stance phase and at the onset of the swing phase, which in turn reduce the metabolic cost of transport of the wearer.

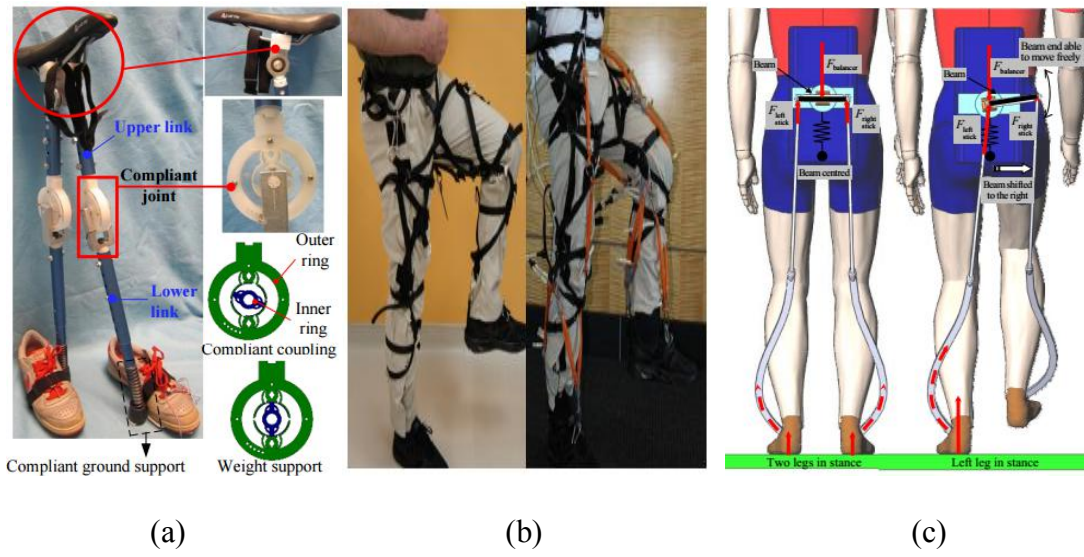


Fig 1.3 (a) LEE (b) Moon-Walker (c) Soft Exosuit

Exoskeleton is always a popular worldwide research topic. For different purposes, many exoskeleton systems with different functions are being built up all over the world, researchers are making efforts on, mechanical design, power supplies, actuators, and transmissions that are lightweight and efficient. Moreover, to make intelligent exoskeleton systems, developments in computing, sensing and control, studies on humans motion are also very important. As a result, the research of exoskeleton combines a lot of knowledge and technologies, and this is why this topic is always interesting, and why researchers in different fields would like to study exoskeleton.

As for suspension system, the suspension system for gravity compensation purpose is not a new topic of research since decades before, the engineers have used different methods to try to remove the gravitational effect on the suspended mass. The mechanism includes band wheel drives, counter weights, linkage with springs. A major application of these kinds of the gravity compensation devices is to attempt to create a zero gravity environment for lab experiments to simulate the environment in space and this is indeed what the devices are built for at first by Joseph et al. 1990. Many researchers keep looking for new possibilities to use this mechanism in different applications. In Chi-Hung Cheng's thesis, a kind of Two Degree-of-Freedom Suspension System was designed, which inspired us of this thesis.



## **1.2 Introduction of Chapters Arrangement**

In the following chapters the mechanism of Two Degree-of-Freedom Suspension System, our exoskeleton system working principal and 3-D model will be introduced. Details of mechanism of suspension system and exoskeleton system will be discussed in Chapter 2. In Chapter 3, the complete exoskeleton model and its working process will be presented. In Chapter 4, the clutch system, thigh release system, which are all for assisting exoskeleton to walk, will be introduced. The final part, Chapter 5, deals with the optimization of back part of our exoskeleton, which is an initial attempt to optimize the whole system that can be developed in the future. The advantage and the most special place of our exoskeleton system compared with other exoskeleton are springs help to hold our body weight just like the suspension system, and the whole system works automatically when led by wearer, without electrical or hydraulic power supply. This means our exoskeleton is combined pure mechanically, the whole system will be light, clean, cheap, easy to build and repair. The capacity of carrying loads will be influenced by springs and stiffness of exoskeleton's material. All in all, by introducing our exoskeleton system, we are hoping to bring out such a concept of building exoskeleton, that is, use mechanical structures as much as possible.

## Chapter 2. Mechanism of 2-D Suspension System and Exoskeleton

### 2.1 Mechanism of 2-D Suspension System

As shown in the Fig 2.1, the system consists of a parallelogram linkage. The links  $l_1$ ,  $l_2$ ,  $l_3$ , and  $l_4$ , provide a two degree-of-freedom system to insure the suspended mass can be moved freely at point C, in a planar work space. Each part is supported by one zero free-length spring. For link #4, the length from the end C to the pivot B and from pivot B to point A are the same ( $l_{41} = l_{42}$ ). The positions of the spring attachment point, F and D, are chosen base on the weight of suspended mass. The point  $O_1$  on the lower left corner of the parallelogram linkage is the origin of the coordinate system. The suspended mass is attached on the upper end C of link #4. It is assumed that the link is uniform, the joints are frictionless.

Since the mass is suspended at point C of the link #4, the length,  $l_{k2}$ , from pivot B to the spring attachment point D can be determined by the moment equation on  $l_4$ :

$$w_a l_{42} \sin \theta_2 - K_2 (l_{s2} - l_{s20}) \sin \varphi_2 l_{41} = 0 \quad (2.1)$$

Where  $w_a$  is the weight of the article attached at point C.

It is also assumed that the spring has zero free-length, the length of the spring #2 before extension,  $l_{s20}$ , is zero. From the geometry, it can be deduced:

$$l_{s2} = \frac{l_{k2} \sin \theta_2}{\sin \varphi_2} \quad (2.2)$$

From (2.1), (2.2), it gives:

$$l_{k2} = \frac{w_a}{K_2} \quad (2.3)$$

Similarly, the moment equation on  $l_1$  can be written as:

$$K_1(l_{s1} - l_{s10})l_1 \sin \varphi_1 - (w_a + m_4 g)l_1 \cos \theta_1 - \left(\frac{m_1}{2}l_1 + \frac{m_2}{2}l_2 + m_3 l_1\right)g \cos \theta_1 = 0 \quad (2.4)$$

With geometry relationship:

$$l_{s1} = \frac{l_{k1} \cos \theta_1}{\sin \varphi_1} \quad (2.5)$$

If spring #1 is zero free-length, and the length of  $l_1$  and  $l_2$  are equal, from (2.4) and (2.5), it gives:

$$l_{k1} = \frac{(m_a + \frac{m_1}{2} + \frac{m_2}{2} + m_3 + m_4)g}{K_1} \quad (2.6)$$

For the case where the inertia of the linkage is zero,

$$l_{k1} = \frac{w_a}{K_1} \quad (2.7)$$

Equations (2.3) and (2.6) show that the force supported by the device can be readily adjusted by changing the lengths  $l_{k1}$  and  $l_{k2}$  for given spring constants  $K_1$  and  $K_2$ .

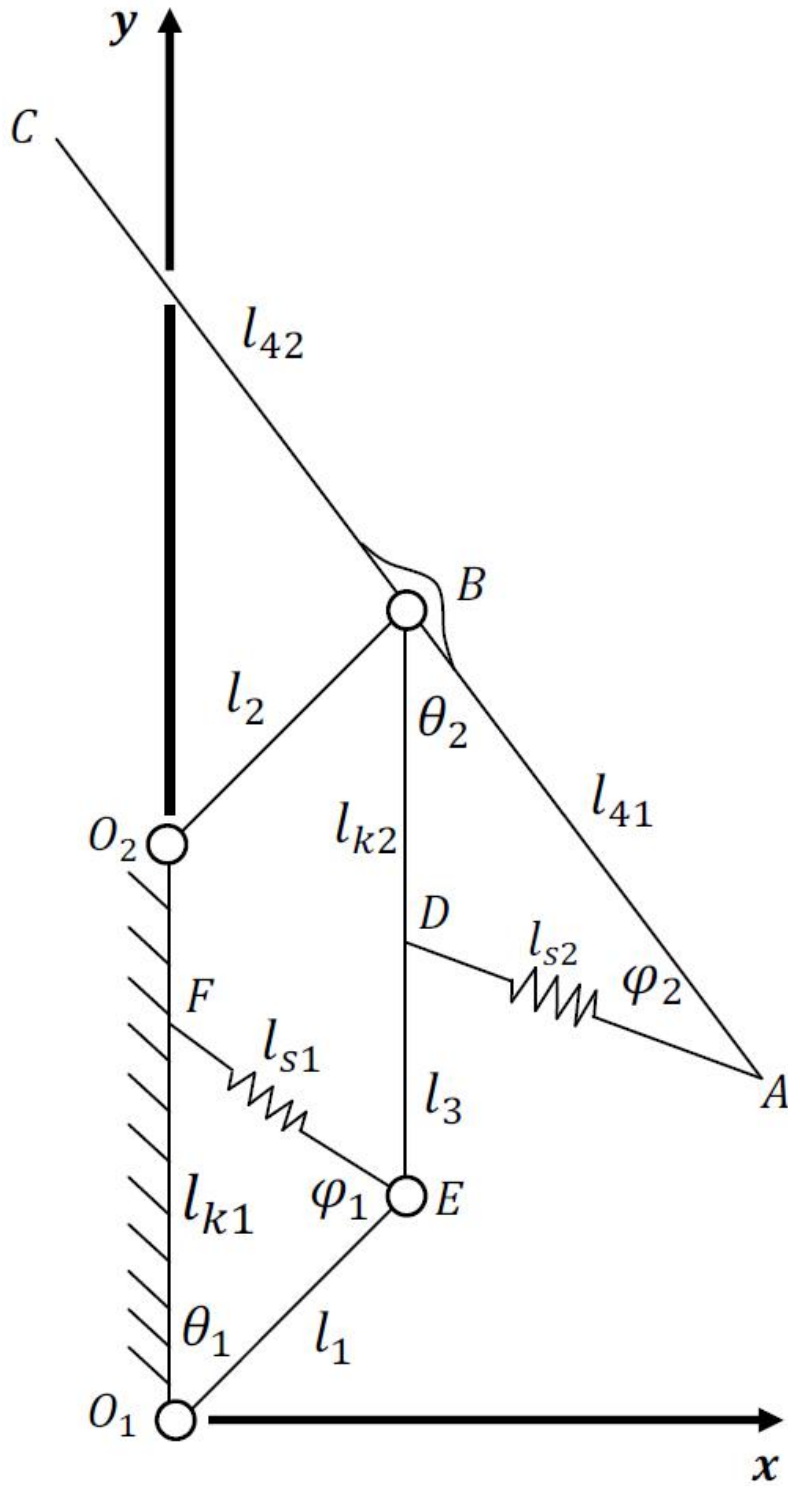


Fig 2.1 Concept of the Two Degree-of-freedom Suspension System from Chi-Hung Cheng's Thesis in 2011

## 2.2 Mechanism of Exoskeleton System

As shown in the Fig 2.2, the exoskeleton system can be seen as an inverted version of lift device.

The working principle is, when people is crouching, the leg is bending, giving an upward force at point C, and  $l_4$  will rotate counterclockwise with the center B.  $l_1$  and  $l_2$  will rotate clockwise with center  $O_1$  and  $O_2$ , respectively. As a result, two springs,  $l_{s1}$  and  $l_{s2}$ , will be extended, they generate forces to drag wearer from a crouching position to straight standing position. During this whole process, wearer can feel much easier to keep a crouching position, because some of his weight are balanced by exoskeletons, especially by the springs.

There are still four main links,  $l_1$ ,  $l_2$ ,  $l_3$ , and  $l_4$ , point E is moved to point E', point D is moved to point E. Moreover,  $l_2$  is connected to wearer's thigh,  $l_{42}$  is connected wearer's shank. B represents wearer's knee,  $\overline{O_1O_2}$  represents wearer's waist and back.

When the exoskeleton provides a force P at point C to support wearer's weight, we have the moment at point B:

$$P \times l_{42} \times \sin \theta_2 - k_2 \times l_{s2} \times l_{41} \times \sin \varphi_2 = 0 \quad (2.8)$$

And the moment at point  $O_1$  :

$$P \times l_1 \times \sin \theta_1 - k_1 \times l_{s1} \times l_1' \times \sin \varphi_1' = 0 \quad (2.9)$$

With geometry relationships:

$$\frac{l_{s1}}{\sin \theta_1} = \frac{l_{k1}}{\sin \varphi_1'} \quad (2.10)$$

$$\frac{l_{s2}}{\sin \theta_2} = \frac{l_3}{\sin \varphi_2} \quad (2.11)$$

Solve (2.8) to (2.11), we have:

$$k_2 = \frac{P \times l_{42}}{l_{41} \times l_3} \quad (2.12)$$

$$k_1 = \frac{P \times l_1}{l_{k1} \times l'_1} \quad (2.13)$$

According to the wearer's height, here we set:

$$l_{41} = 12\text{cm}$$

$$l_{42} = 54\text{cm}$$

$$l_3 = 16\text{cm}$$

$$l_1 = 60\text{cm}$$

$$l'_1 = 40\text{cm}$$

$$l_{k1} = 8\text{cm}$$

If we need a force, P equals to 200N, we can calculate the springs rate by (2.12) and (2.13):

$$k_1 = 3.75\text{N/cm}$$

$$k_2 = 5.63\text{N/cm}$$

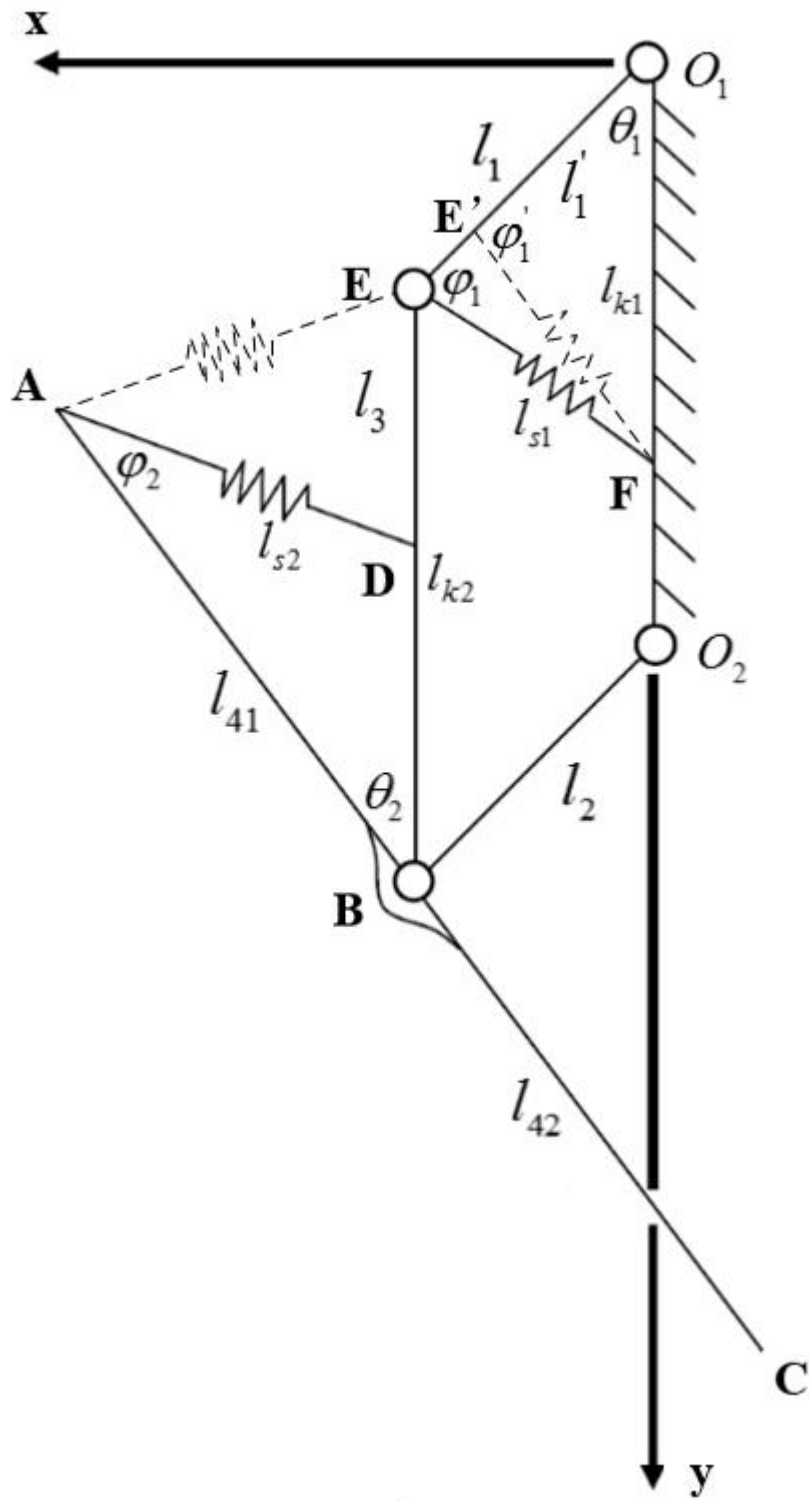


Fig 2.2 Concept of the exoskeleton system

## Chapter 3. 3-D Model of Exoskeleton

### 3.1 Introduction of 3-D Model of Exoskeleton

As shown in Fig 3.1, it is a whole basic 3-D model of the exoskeleton, which is built up by Solidworks. Considering the system's symmetry, to be more concise and convenience, only one side structure of the system will be introduced through Fig 3.2. As shown in Fig 3.2, main components of right side of the exoskeleton are indicated with numbers. These numbers' meaning are:

- 1: back plate of the exoskeleton
- 2: weight support springs( $l_{s1}$  and  $l_{s2}$ )
- 3: waist belt
- 4, 17: vertical linkages( $l_3$ )
- 5, 6, 9, 11, 15: pulleys
- 7: red cable
- 8: green cable
- 10, 16: hooks
- 12: thigh wrap
- 13, 14: thigh linkages( $l_1$  and  $l_2$ )
- 18: shank wrap
- 19: shank linkage( $l_4$ )



In 3-D model, the parallelogram structure includes vertical linkages, thigh linkages and shank linkage, which are connected with bearings. Notably, we change the position of  $l_{s1}$  and  $l_{s2}$ , this is because  $l_{s1}$  and  $l_{s2}$  are going to support part of wearer's weight, thus the extension forces in  $l_{s1}$  and  $l_{s2}$  will be big. As a result, quite long springs with suitable rate are chosen, so we need to move the springs from original positions to backside of the exoskeleton. Because we only change the direction of extension forces in springs by using several pulleys, so the movement of springs' position will not contravene the basic mechanism.

The exoskeleton can be connected to the wearer by waist belt, thigh wraps and shank wraps, which are built by fabric material. To help transfer the body weight to back springs, we mainly use two cables, red cable and green cable. The red cable starts from the hook on shank linkage, comes through a series pulleys, such as 15, 11, 9 and 6, connected with one of springs. The green cable starts from the hook on thigh linkage, comes through pulleys 9 and 5, connected with the other one spring.

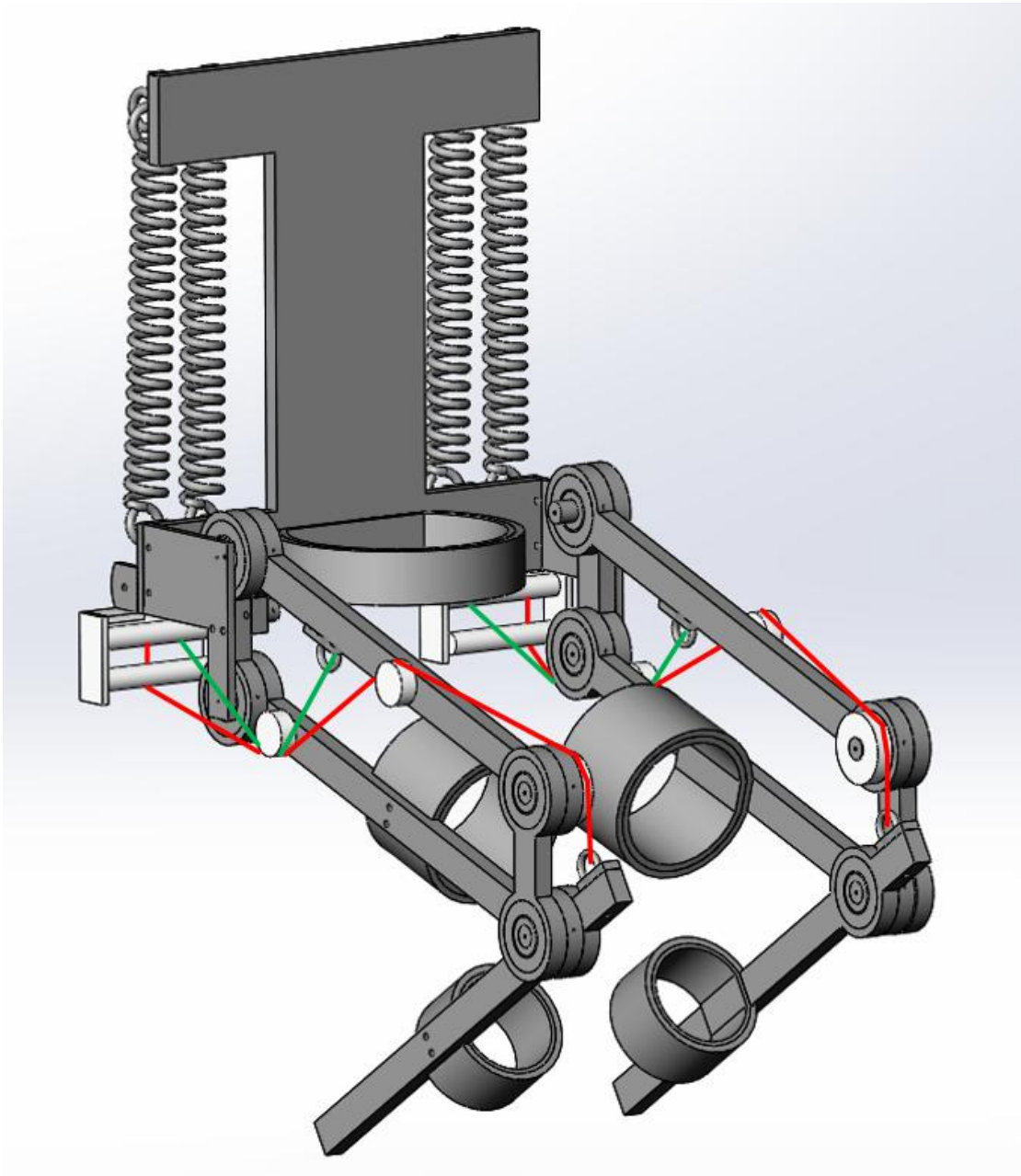


Fig 3.1 Basic 3-D model of exoskeleton in Solidworks

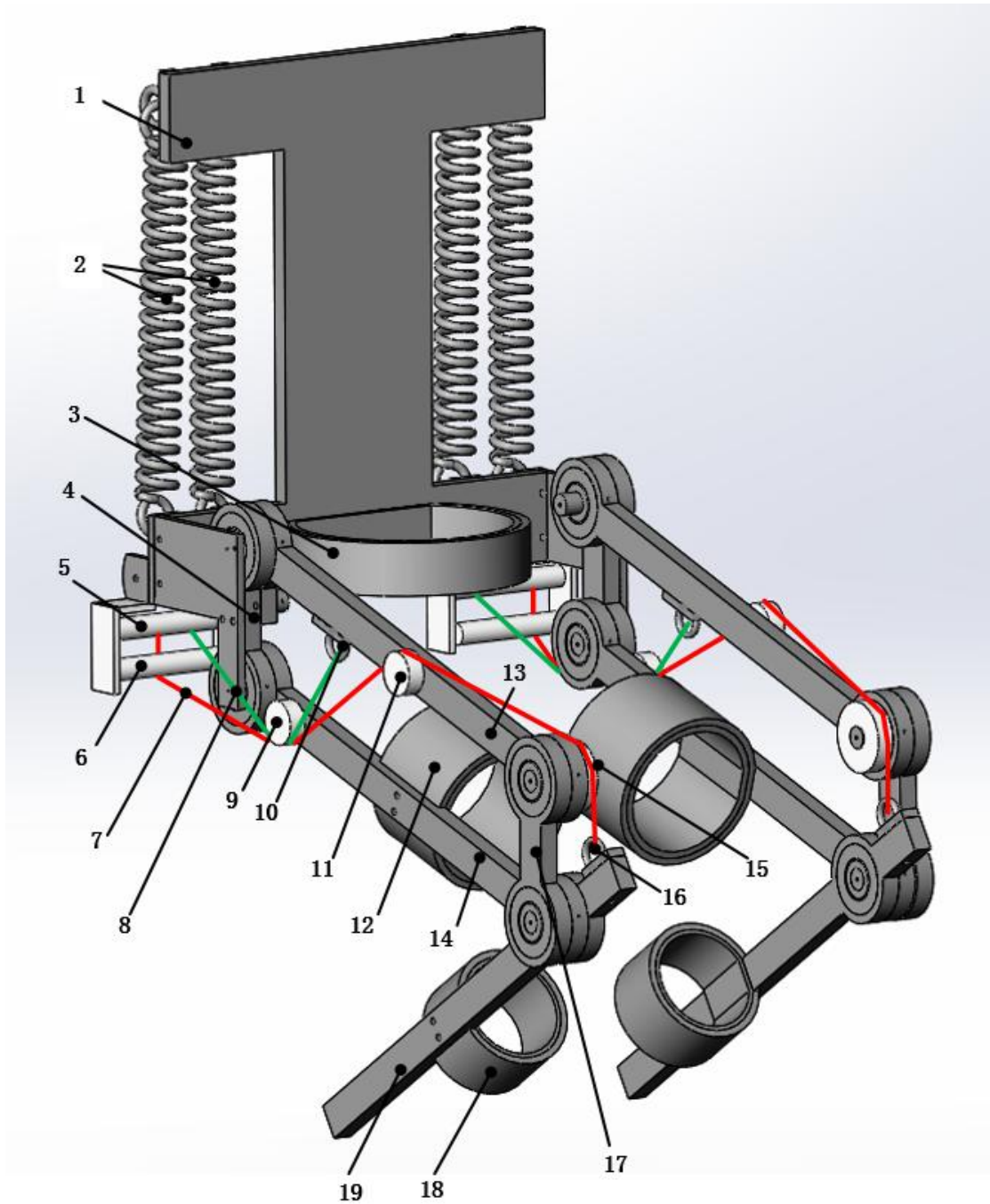


Fig 3.2 Basic 3-D model of exoskeleton in Solidworks  
(main components indicated)

### **3.2 Working Principle of 3-D Exoskeleton**

We will talk about the working principle of the exoskeleton by introducing two main stages of the exoskeleton, and how the related components move. Before the introduction, we need to notice that the linkages and legs are connected by wraps, so the linkages will move in the same way led by legs.

As shown in Fig 3.3, at the first stage, which we call the standing stage, the wearer is standing nearly straight, so the exoskeleton is also nearly straight. At this stage the backside springs are not extended and thus they do not hold the weight of the wearer. Then the wearer begins to crouch, at this time the shank linkage will rotate clockwise, the thigh linkage will come upwards, then there would be extension forces in red cable and green cable, respectively. These forces pass through the cables and at last come to the springs, thus the springs change from free stage to extension stage. Here it comes to the second stage, which we call the crouching stage, as shown in Fig 3.4. With the help of the extension forces in the springs, the exoskeleton is able to exert forces at wearer's shank and thigh, to drag the wearer's back to stand straight.

At last, some of the wearer's weight can be balanced by the drag force, in this way we can say the exoskeleton is able to support the wearer's weight, to help the wearer feel much more easier when he or she keeps a crouching position.

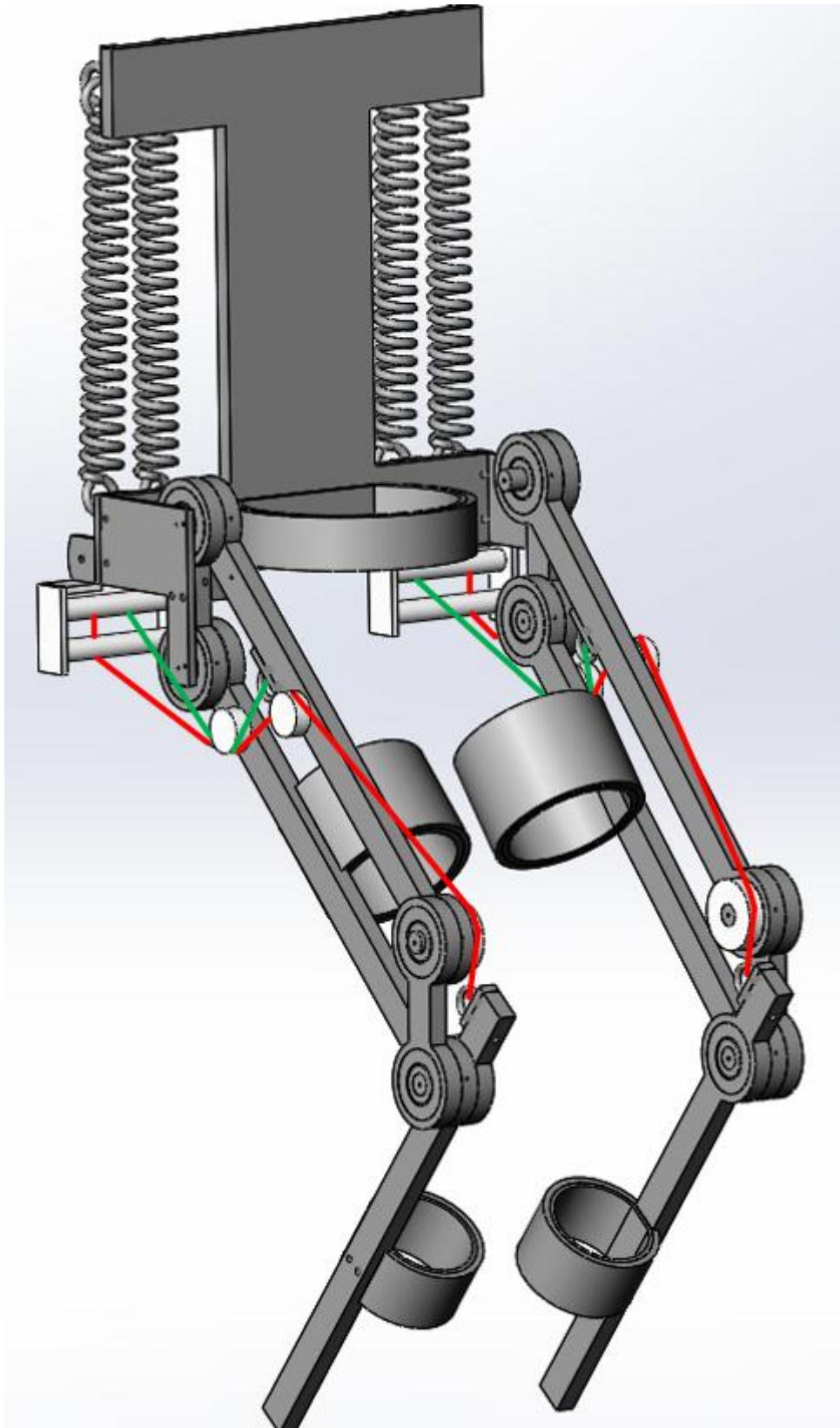


Fig 3.3 The exoskeleton at standing stage

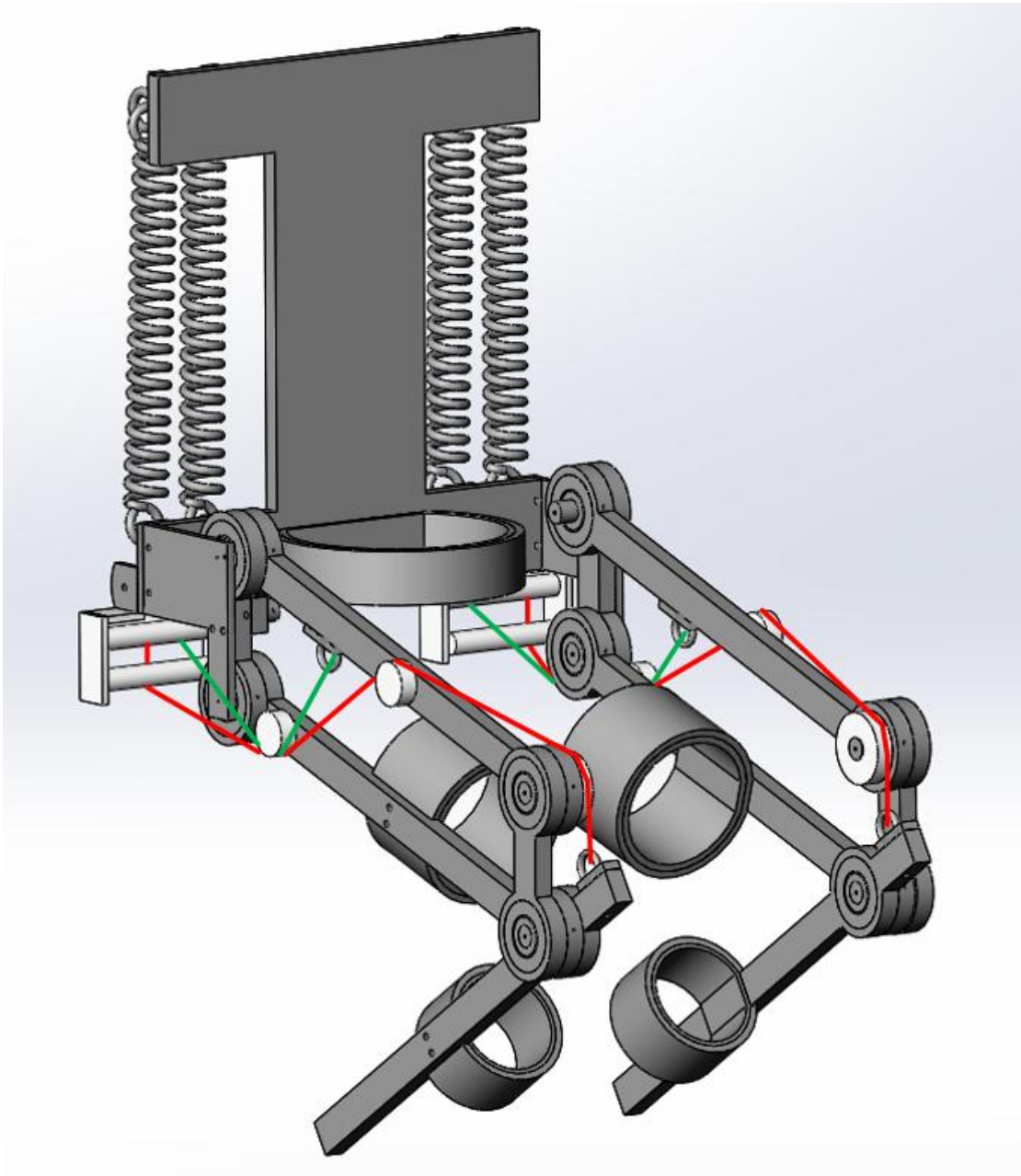


Fig 3.4 The exoskeleton at crouching stage

## Chapter 4. Walking Assistive Systems in Exoskeleton

### 4.1 Introduction of Clutch System

In Chapter 3, we can see the exoskeleton is able to help wearer keep a crouching position easily. In order to enrich our research and give the exoskeleton more functions, we wish to make the exoskeleton able to walk when led by a walking wearer. To achieve this goal, a clutch system and a cable release system are designed. In this part we will mainly talk about clutch system, and cable release system will be discussed in next part.

As shown in Fig 4.1, it is a 3-D model of clutch system. The main components of the clutch system are indicated with numbers, specifically, these numbers represent:

1: base plate

2: bottom plate a

3: ratchet a

4: axis a

5: rod a

6: bottom plate b

7: ratchet b

8: axis b

9: rod b

10: bottom plate c

11: axis c

12: ratchet c

13: green cable

14: spring a

15: pin a

16: axis d

17: spring b

18: pin b

19: axis e

20: spring c

21: pin c

22: pulley a

23: axis f

24: brown cable

25: pin d

26: red cable



The base plate is fixed, bottom plates, ratchets, pulley and pins are mainly connected on different axis, which are fixed on base plate. Ratchet a and bottom plate a can rotate separately, ratchet b and bottom plate b can also rotate separately, but ratchet c and bottom plate c are one piece, so they can rotate together. Pin a, b and c are connected with pin a, b and c with spring a, b and c, respectively. Rod a and b connect bottom plate a and b, bottom plate b and c, respectively. Brown cable connects pin c and pin d through a pulley.

Another thing we need to notice is that, the green cable connects thigh linkage and backside spring, and it is also connected with ratchet a. The red cable connects shank linkage backside spring, and it is also connected with ratchet b and bottom plate c.

To introduce the working principle of clutch system, we need to focus on different stages of walking. At the original stage(Fig 4.1), wearer and exoskeleton are at a crouching position, there will be extension forces in springs and cables. When the wearer is going to walk, at first he or she should bend his or her leg a little more, at this time the red cable will be dragged to move rightward, led by the red cable, bottom plate c and ratchet c will rotate clockwise, thus pin d will lead the brown cable to pull pin c away from ratchet c. As bottom plate c and ratchet rotate clockwise, rod b will drag the pin of bottom plate b to come down until it stuck on pin b, then they come down together until pin b stuck on ratchet b. At the same time, with similar movement process, rod a drags the pin of bottom plate a to come down until it stuck on pin a, then they come down together until pin a stuck on ratchet a. Here as a result, the ratchets a and b cannot rotate, so the green cable and red cable cannot move, as well

as the backside springs' length. At this stage, as shown in Fig 4.2, because the green cable, red cable and ratchets a and b are locked, we say this stage is lock stage. When the clutch system comes to lock stage, the wearer can lift his or her leg to walk.

As the wearer lift his or her leg to walk, namely, one of the wearer's leg is in the air, the clutch system also keeps staying lock stage. When the wearer finishes one step, his or her feet are both on the ground, the clutch system can be unlocked. To unlock the clutch system, the wearer needs to stand a little straight but still stay at a crouching position. During this process, the red cable will move leftward, bottom plate c and ratchet c rotate counterclockwise, pin c comes back to stuck on the ratchet c. Meanwhile, rod a and b will push bottom plate a and b, make them rotate counterclockwise, thus pin a and b will be released to leave ratchet a and b, then they will be dragged by spring a and b to come back to original position, respectively. Finally, the clutch system comes back to the original stage, and wearer is at crouching position again, ready for walking next step.

Besides assisting people to walk, the clutch system can also prevent legs being hurt by backside springs. This is because when wearer is crouching, the backside springs are holding some of wearer's weight, thus the forces in them will be quite large, about 20lbs to 30 lbs for each spring. If we don't use clutch system, at the moment the wearer lift his or her leg to move forward, the forces in backside springs will suddenly drag the leg to go backward until there is no extension length in the springs. The sudden force and acceleration exerted on the leg will hurt the leg, which will not be allowed. With the clutch system, as wearer lift his or her leg, the cables linked with

springs are locked, so the springs' length will not change, and there would be no sudden force and acceleration exerted on the leg. As a result the wearer's leg is protected.

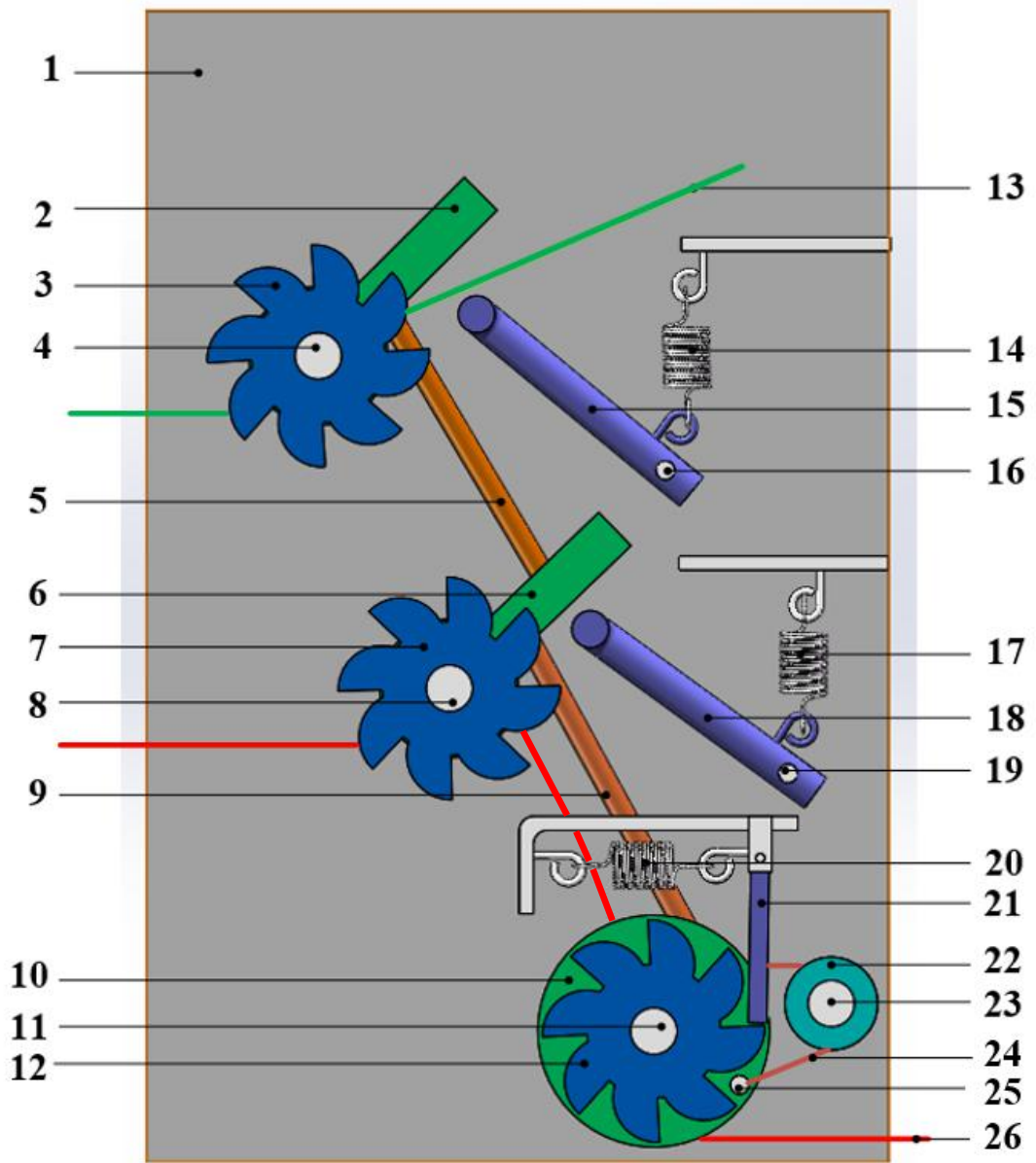


Fig 4.1 3-D model of clutch system at original stage

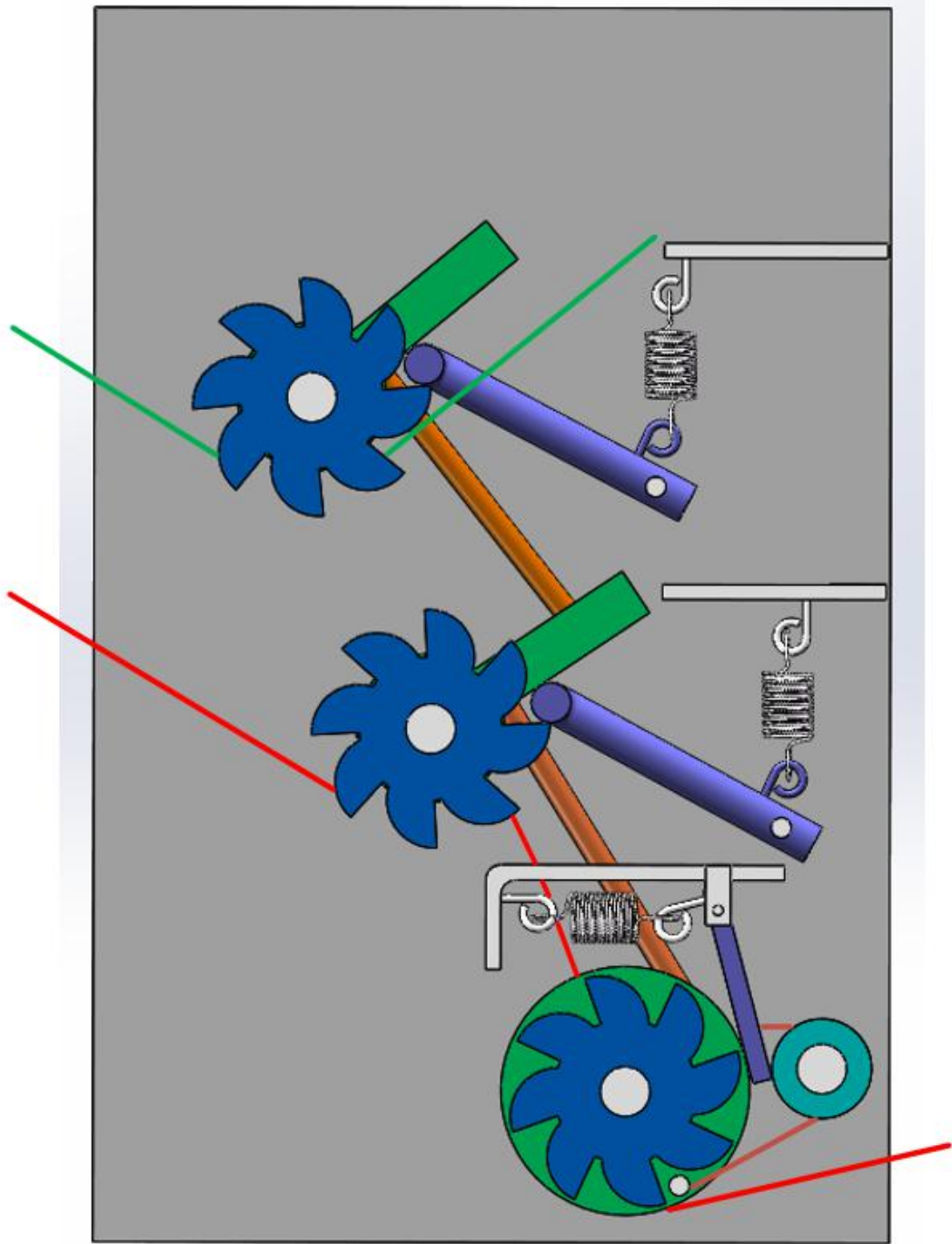


Fig 4.2 3-D model of clutch system at lock stage

## 4.2 Introduction of Cable Release System

We need to notice that after the clutch system is locked, in order to walk, the wearer needs to lift one of his or her thigh at first. The problem is, at this time, the cable which links thigh linkage and backside spring, is locked, there would be no extra length for lifting wearer's thigh. Thus it is necessary to design a cable release system to provide enough length cable for lifting wearer's thigh.

As shown in Fig 4.3, it is a 3-D model of cable release system. The main components of the system are indicated with numbers:

- 1: bottom base plate
- 2: connection bar
- 3: spring a and b (two springs, the other one can be seen in side view)
- 4: pulley
- 5: green cable
- 6: axis of pulley
- 7: axis lead rail
- 8, 9: magnets
- 10: bar of pulley
- 11: spring c
- 12: lead rail connection bar

The bottom base plate is connected with the base plate of clutch system, springs a and b link connection bar and axis of pulley. The green cable, which connects clutch system and thigh linkage, comes through the pulley. The lead rail is fixed on the bottom plate by connection bar. And spring c is linked with the bar of pulley and pin a of the clutch system, which can be seen in Fig 4.5.

To introduce the working mechanism of cable release system, we need to focus on force analysis, and a series working stages of the system. Here we set:

$F_t$  : extension force in green cable

$F_{sa}$  : extension force in spring a

$F_{sb}$  : extension force in spring b

$F_{sc}$  : extension force in spring c

$F_m$  : attract force in magnets

The other related parameters are all indicated in Fig 4.3.

At the beginning stage, namely, the unlock stage, the bar of pulley is attracted by magnets, until they split up we have:

$$F_t \times \cos \theta_1 + F_t \times \cos \theta_2 + F_{sc} - F_{sa} - F_{sb} - F_m = 0 \quad (4.1)$$

When the wearer begin to bend to lock the clutch system, as the pin a of the clutch system goes downward, spring c will be extended to drag the bar of pulley, when the extension force in spring c is big enough, the bar of pulley will leave the magnets, the whole pulley will come downward as well. At this time, the clutch system is locked, the green cable will be loose, so the wearer is able to lift his or her leg, then to step forward.

By defining spring rate of spring a, b and c, we are able to determine the new balance position of the pulley, which is shown with blue dash circle in Fig 4.3, the new position of green cable is also shown with green dash line in Fig 4.3.

The total released length of cable is:

$$l_r = l_1 + l_2 - l_1 \times \cos \theta_1 - l_2 \times \cos \theta_2 \quad (4.2)$$

The spring rate of spring a, b and c:

$$k_a = k_b = \frac{F_{sa}}{h} = \frac{F_{sb}}{h} \quad (4.3)$$

$$k_c = \frac{F_{sc}}{h} \quad (4.4)$$

We set the values of parameters as follows to satisfy (4.1):

$$F_t = 20lbs$$

$$F_{sa} = F_{sb} = 10lbs$$

$$F_{sc} = 10lbs$$

$$F_m = 20lbs$$

And if we set:

$$l_1 = l_2 = 6\sqrt{2}cm, \quad h = 6cm, \quad d_1 = d_2 = 6cm, \quad \theta_1 = \theta_2 = 45^\circ,$$

By substitute these numbers in (4.1) to (4.4), we have:

$$l_r = 5cm,$$

$$k_a = k_b = 4.2lbs / inch, \quad k_c \geq 4.2lbs / inch \quad \text{with suitable length.}$$



Moreover, if we set:

$$l_1 = l_2 = 12cm, \quad h = 6\sqrt{3}cm, \quad d_1 = d_2 = 6cm, \quad \theta_1 = \theta_2 = 30^\circ$$

With similar calculation we have:

$$l_r = 12cm,$$

$$k_a = k_b = 3.1lbs / inch, \quad k_c \geq 2.5lbs / inch \quad \text{with suitable length.}$$

Or if we set:

$$l_1 = l_2 = 8\sqrt{2}cm, \quad h = 8cm, \quad d_1 = d_2 = 8cm, \quad \theta_1 = \theta_2 = 45^\circ$$

With similar calculation we have:

$$l_r = 6.6cm,$$

$$k_a = k_b = 3lbs / inch, \quad k_c \geq 3lbs / inch, \quad \text{with suitable length.}$$

By measurement, a 5cm released cable length is enough for wearer's one foot long step. And by changing related parameters, we are able to adjust the released cable length to better serve the wearer.

The combination of cable release system and clutch system, which we call walking assistive systems, can be seen in Fig 4.5. And the assemble of walking assistive systems and the exoskeleton can be seen in Fig 4.6, the details in the dash frame of Fig 4.6 can be seen in Fig 4.7.

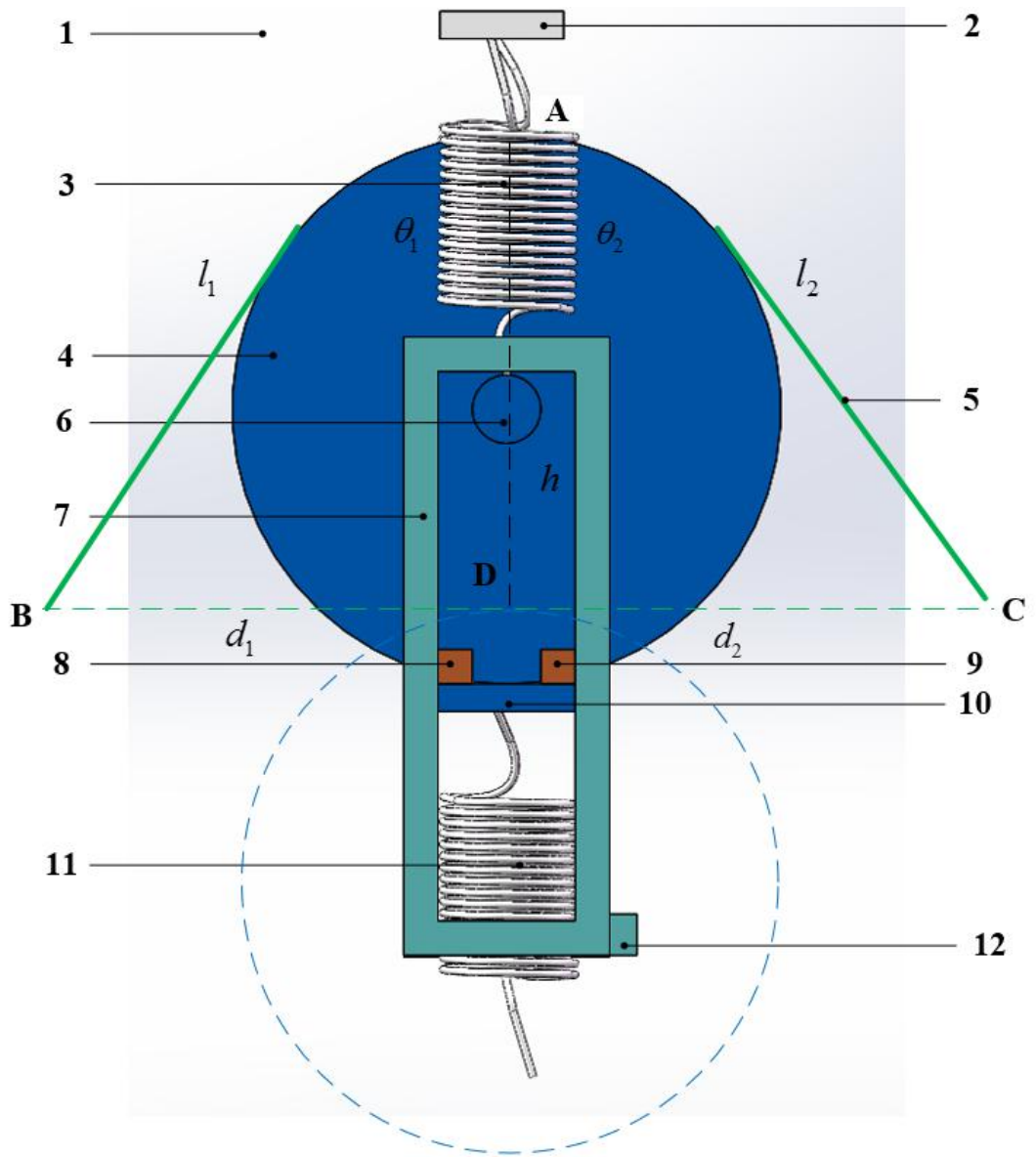


Fig 4.3 3-D model of cable release system

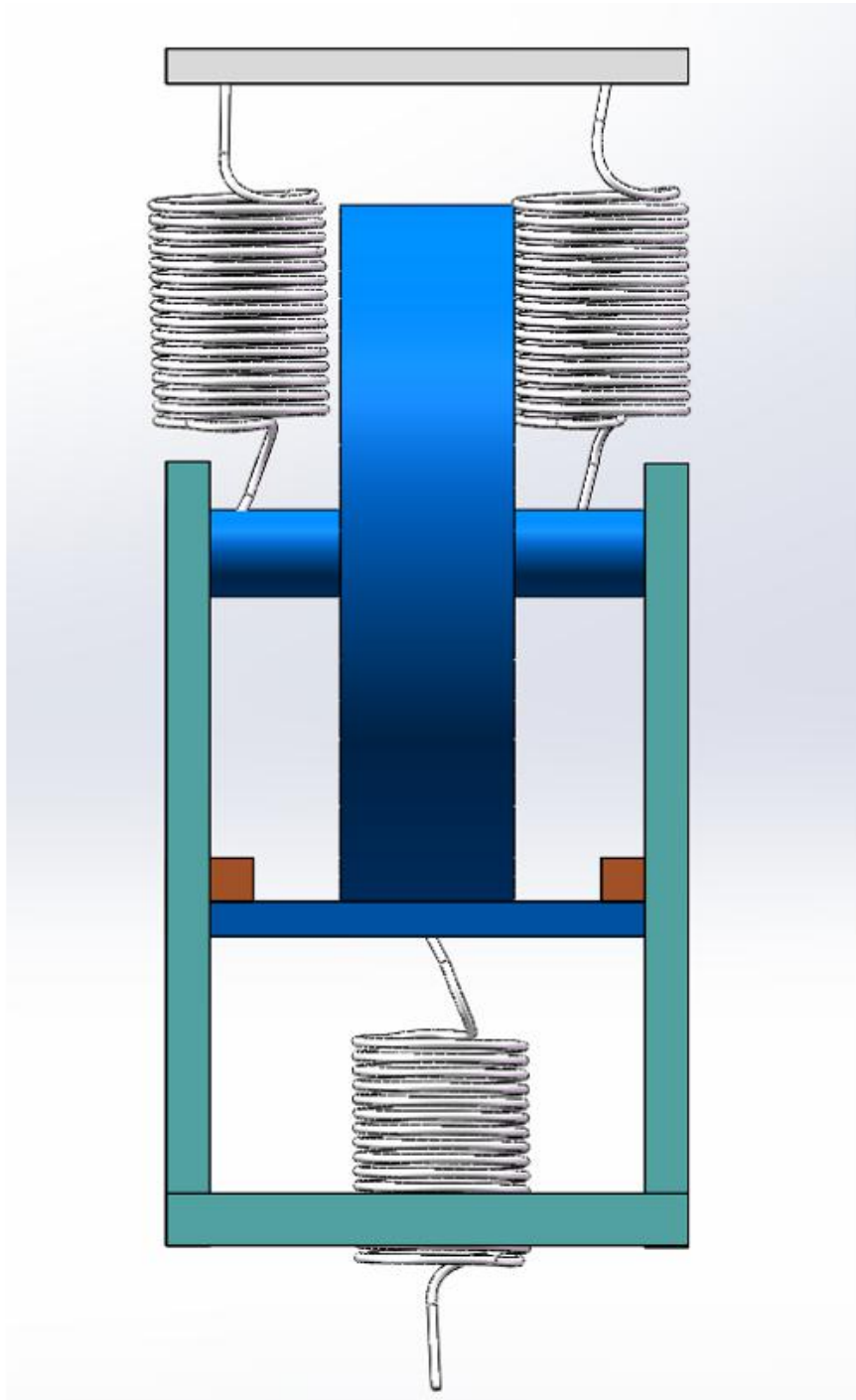


Fig 4.4 Side view of cable release system

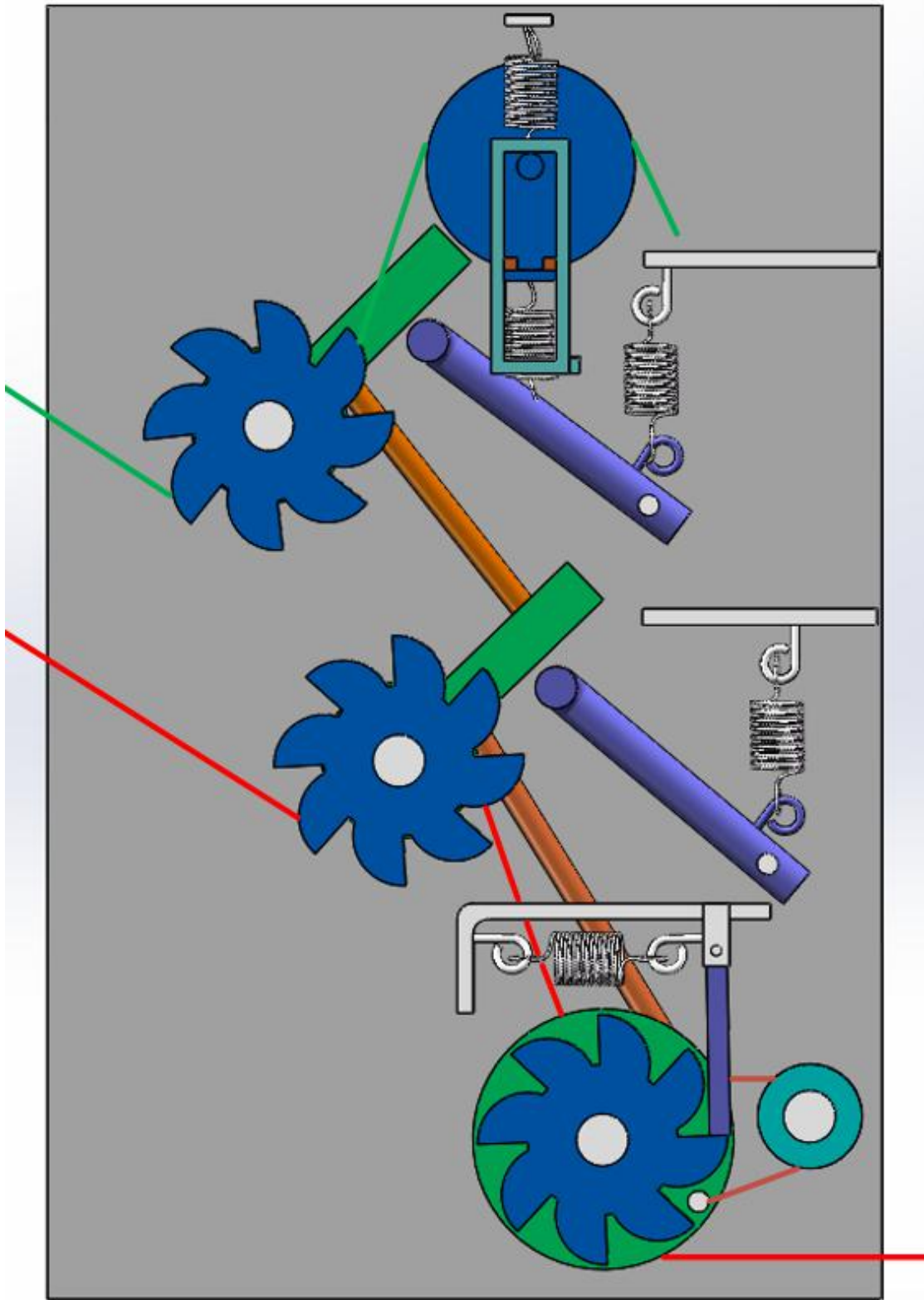


Fig 4.5 3-D model of walking assistive system

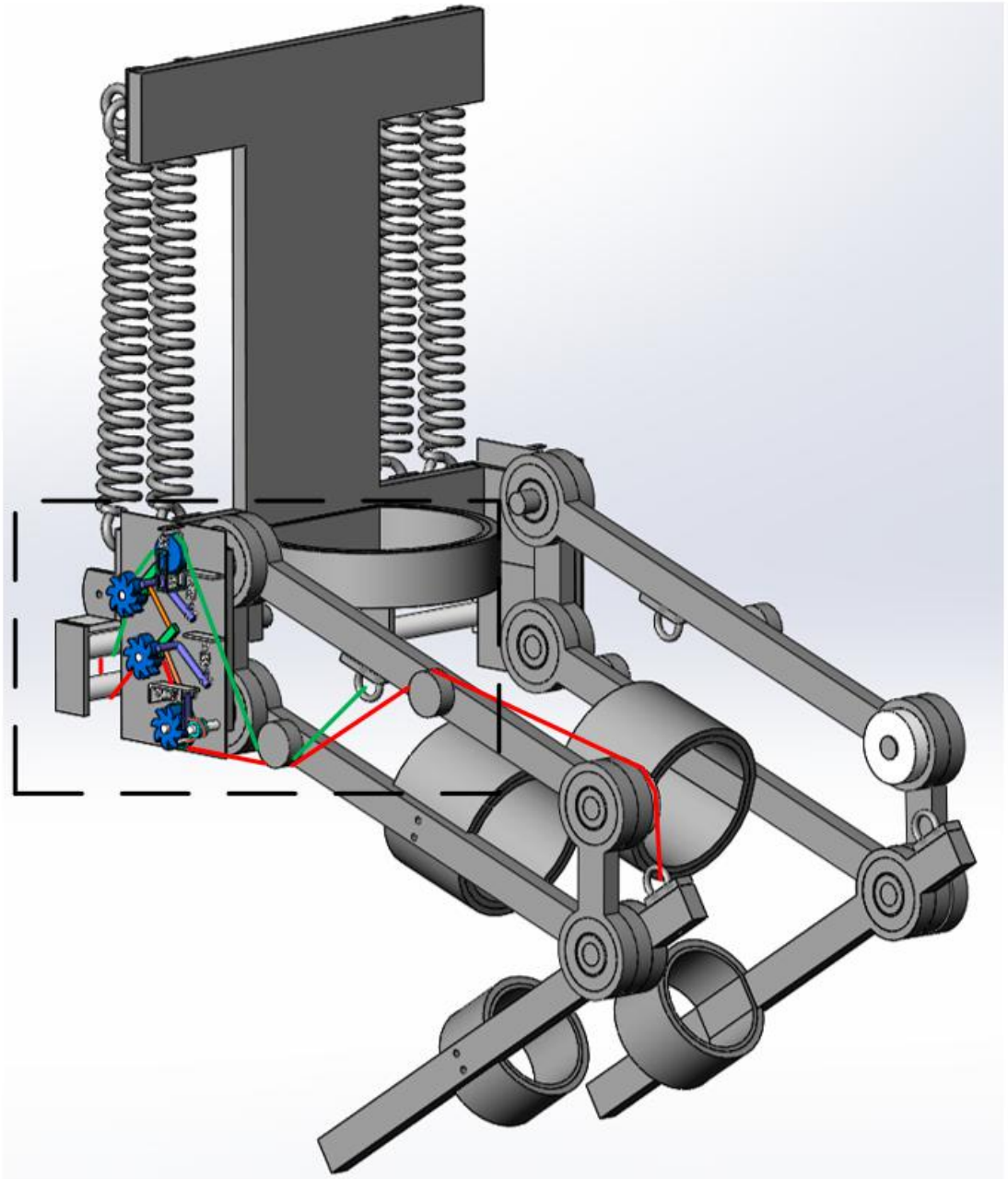


Fig 4.6 3-D model of whole exoskeleton system

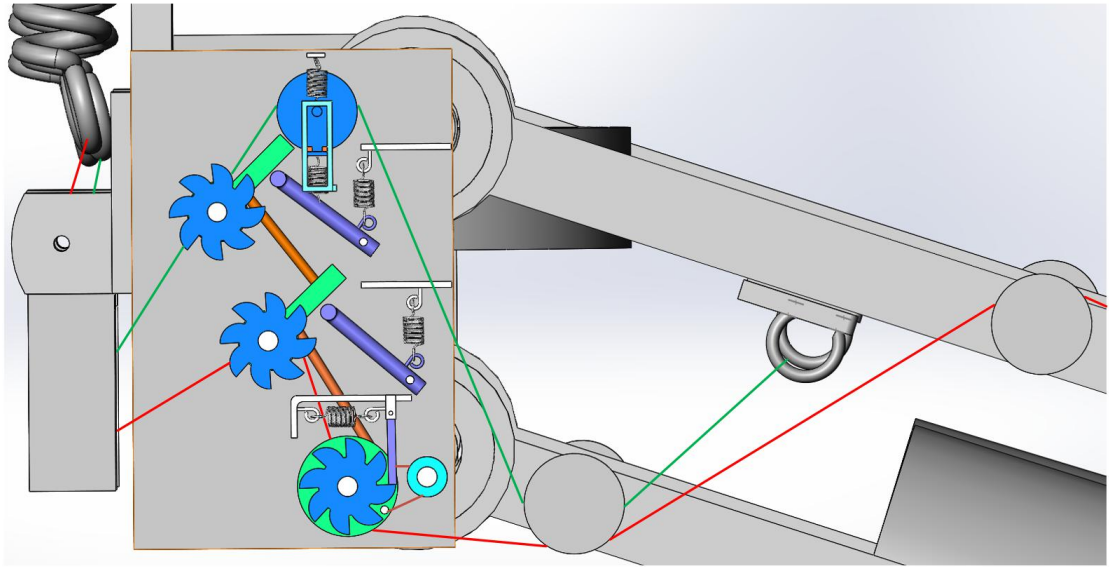


Fig 4.7 walking assistive system in the whole exoskeleton system

## Chapter 5. Two Dimensional Shape Optimization of Back Part in Exoskeleton

### 5.1 Introduction of Topology Optimization

As last Chapter of this thesis, we want to explore applied optimization technique in designing our exoskeleton, which could also be one of direction of our future research.

As an important part, the back part of exoskeleton needs to be considered carefully. In this Chapter we use a 99 line topology optimization code as a base, by constructing a simple model, revising the code, we want to obtain an ideal two-dimensional shape of our backside exoskeleton.

A topology optimization problem based on the power-law approach, where the objective is to minimize compliance can be written as

$$\left. \begin{aligned} \min_{\mathbf{x}} : c(\mathbf{x}) &= \mathbf{U}^T \mathbf{K} \mathbf{U} = \sum_{e=1}^N (x_e)^p \mathbf{u}_e^T \mathbf{k}_0 \mathbf{u}_e \\ \text{subject to : } \frac{V(\mathbf{x})}{V_0} &= f \\ &: \mathbf{K} \mathbf{U} = \mathbf{F} \\ &: \mathbf{0} < \mathbf{x}_{\min} \leq \mathbf{x} \leq \mathbf{1} \end{aligned} \right\} ,$$

where  $\mathbf{U}$  and  $\mathbf{F}$  are the global displacement and force vectors, respectively,  $\mathbf{K}$  is the global stiffness matrix,  $\mathbf{u}_e$  and  $\mathbf{k}_e$  are the element displacement vector and stiffness matrix, respectively,  $\mathbf{x}$  is the vector of design variables,  $\mathbf{x}_{\min}$  is a vector of minimum relative densities (non-zero to avoid singularity),  $N (= n_{elx} \times n_{ely})$  is the number of elements used to discretize the design domain,  $p$  is the penalization power (typically  $p$

= 3),  $V(x)$  and  $V_0$  is the material volume and design domain volume, respectively and  $f(\text{volfrac})$  is the prescribed volume fraction.

The Matlab code (see the Appendix), is built up as a standard topology optimization code. The main program is called from the Matlab prompt by the line:

**top ( nelx , nely , volfrac, penal ,rmin ).**

where  $\text{nelx}$  and  $\text{nely}$  are the number of elements in the horizontal and vertical directions, respectively,  $\text{volfrac}$  is the volume fraction,  $\text{penal}$  is the penalization power and  $\text{rmin}$  is the filter size (divided by element size). Other variables as well as boundary conditions are defined in the Matlab code itself and can be edited if needed. For each iteration in the topology optimization loop, the code generates a picture of the current density distribution.

The main program (lines 1–36) starts by distributing the material evenly in the design domain (line 4). After some other initializations, the main loop starts with a call to the Finite Element subroutine (line 12) which returns the displacement vector  $U$ . Since the element stiffness matrix for solid material is the same for all elements, the element stiffness matrix subroutine is called only once (line 14). Following this, a loop over all elements (lines 16–24) determines objective function and sensitivities (4). The variables  $n_1$  and  $n_2$  denote upper left and right element node numbers in global node numbers and are used to extract the element displacement vector  $U_e$  from the global displacement vector  $U$ . The sensitivity analysis is followed by a call to the mesh-independency filter (line 26) and the Optimality Criteria optimizer (line 28). The current compliance as well as other parameters are printed by lines 30–33 and the



resulting density distribution is plotted (line 35). The main loop is terminated if the change in design variables (change determined in line 30) is less than 1percent2. Otherwise above steps are repeated.

The updated design variables are found by the optimizer (lines 37–48). Knowing that the material volume ( $\text{sum}(\text{sum}(\text{xnew}))$ ) is a monotonously decreasing function of the Lagrange multiplier (lag), the value of the Lagrangian multiplier that satisfies the volume constraint can be found by a bi-sectioning algorithm (lines 40-48). The bi-sectioning algorithm is initialized by guessing a lower  $l_1$  and an upper  $l_2$  bound for the Lagrangian multiplier (line 39). The interval which bounds the Lagrangian multiplier is repeatedly halved until its size is less than the convergence criteria (line-40).

Lines 49–64 represent the Matlab implementation of (5). Note that not all elements in the design domain are searched in order to find the elements that lie within the radius  $r_{min}$  but only those within a square with side lengths two times  $\text{round}(r_{min})$  around the considered element. By selecting  $r_{min}$  less than one in the call of the routine, the filtered sensitivities will be equal to the original sensitivities making the filter inactive.

The finite element code is written in lines 65–99. Note that the solver makes use of the sparse option in Matlab. The global stiffness matrix is formed by a loop over all elements (lines 70–77). As was the case in the main program, variables  $n_1$  and  $n_2$  denote upper left and right element node numbers in global node numbers and are used to insert the element stiffness matrix at the right places in the global stiffness

matrix. The element stiffness matrix is calculated in lines 86–99. The 8 by 8 matrix for a square bi-linear 4-node element was determined analytically using a symbolic manipulation software. The Young's modulus  $E$  and the Poisson's ratio  $\nu$  can be altered in lines 88 and 89.

The main code part is introduced as above, many conditions such as fixeddofs, freedofs, value and direction of force, Young's modulus  $E$  and Poisson's ratio etc. can be changed due to different problems.

## 5.2 Application of Topology Optimization in Exoskeleton

Fig 5.1 shows our basic two-dimensional model of back part exoskeleton, its original shape is a  $500 \times 600$  rectangular block, ignoring its thickness. Sizes are indicated in Fig 5.1, the bottom side of the block is constrained, and  $F_1 = F_2 = F_3 = F_4 = 1000N$ . What we need to do is express our model in topology optimization 99 line code.

The size of the back part exoskeleton, forces' position, value, direction, and boundary fixed and free conditions are all shown in Fig 5.1. The reason why we choose the bottom side of the block to be fixed is because in our real exoskeleton, this part is connected with waist part and thigh part, in our design principle, these parts' connection should not move, this is the key how the whole exoskeleton system works. So, as the connection side, the bottom side of the model, shown as Fig 5.1, should be fixed.

For convenience calculation, we set  $100 \times 120$  grids in our simulation progress. Choose volume rate as 0.5, 0.6, 0.7, 0.8, 0.9, to get the result with largest stiffness in corresponding condition, respectively.

One more thing we need to mention here is five parameters we need to determine at first,  $nelx$ ,  $nely$ ,  $volfrac$ ,  $penal$ ,  $rmin$ , which are grids in x direction, grids in y direction, volume rate, penal coefficient, filter size.

In code, usually we set Young modulus  $E=1$ , force  $F=-1$ (if not indicated), Poisson ratio  $\nu=0.3$ . (if  $\nu$  is too large, the matrix calculation will go wrong). The results can be seen in Fig 5.2.

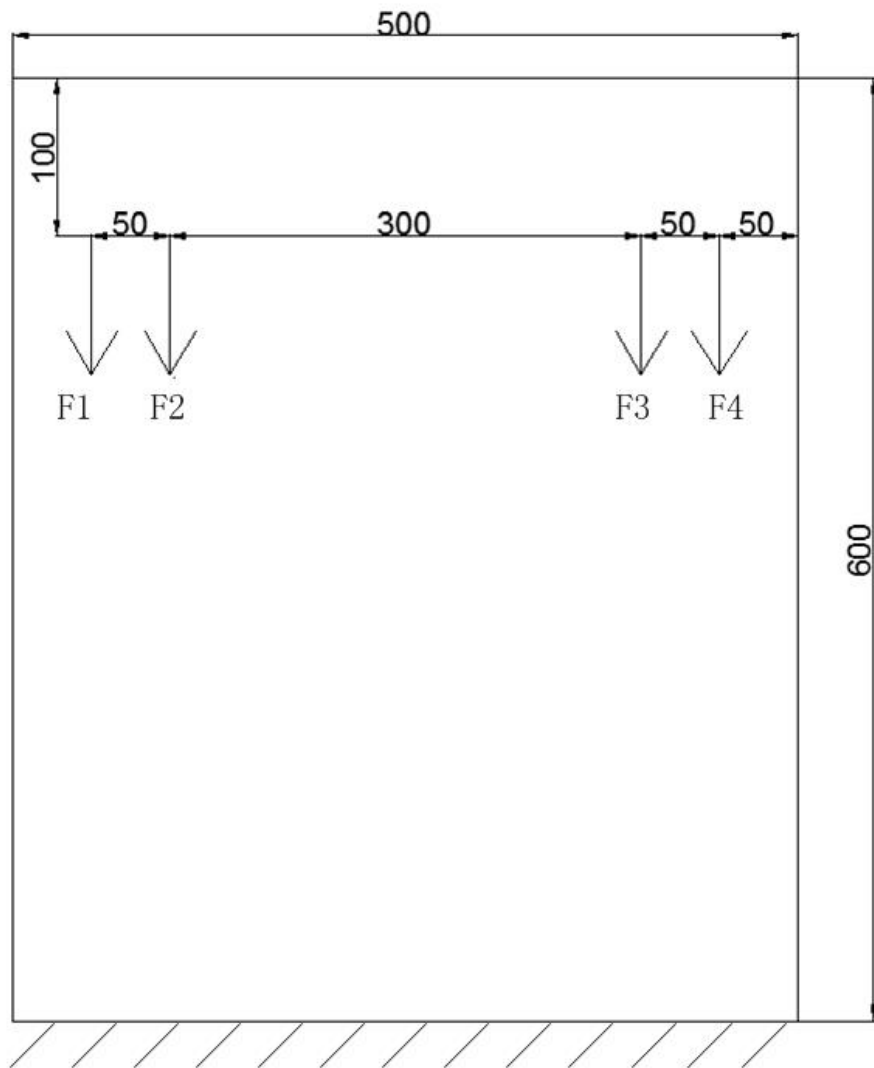
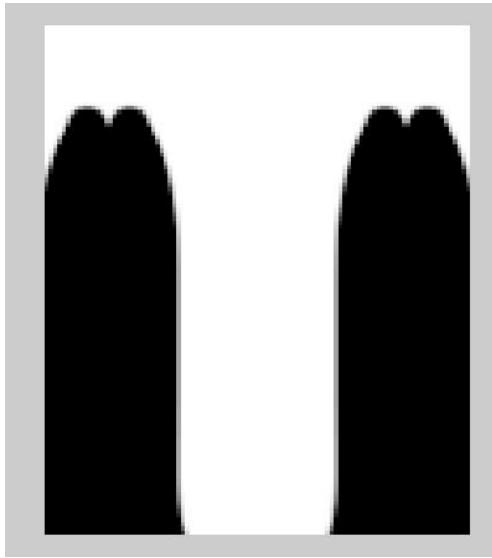
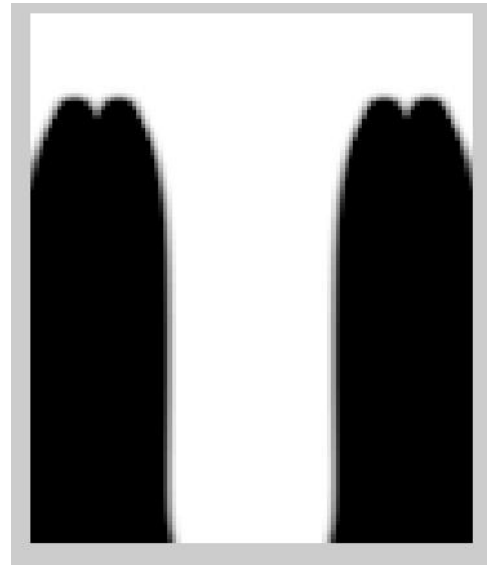


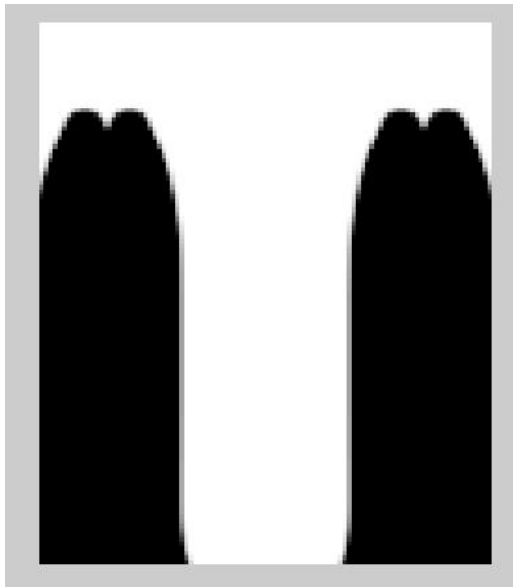
Fig 5.1 Two-dimensional model of back part exoskeleton



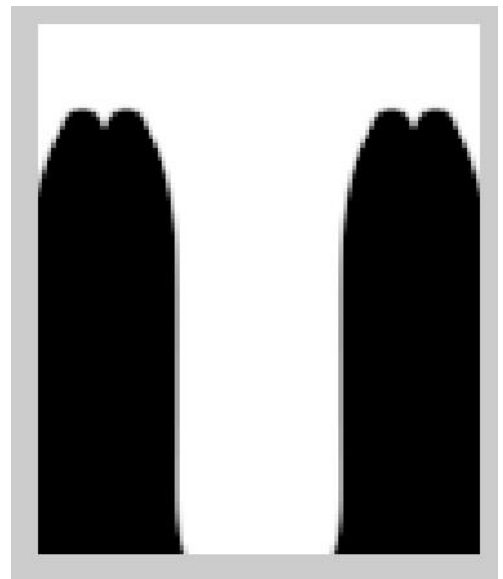
(a) 100,120,0.5,3,1.5



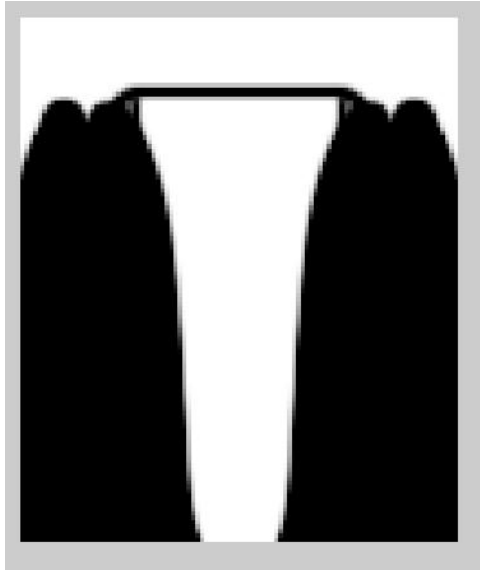
(b) 100,120,0.5,3,3



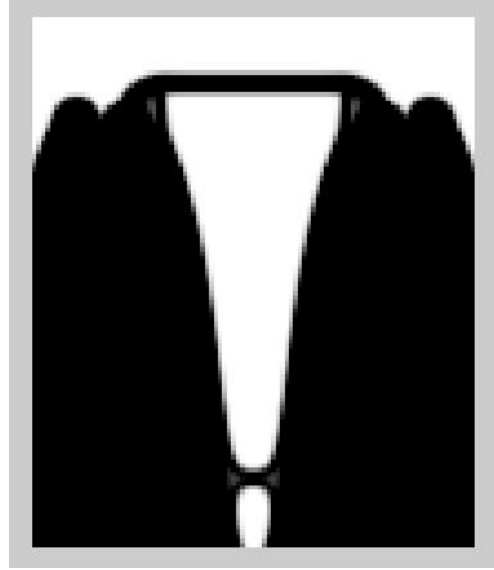
(c) 100,120,0.5,4,1.5



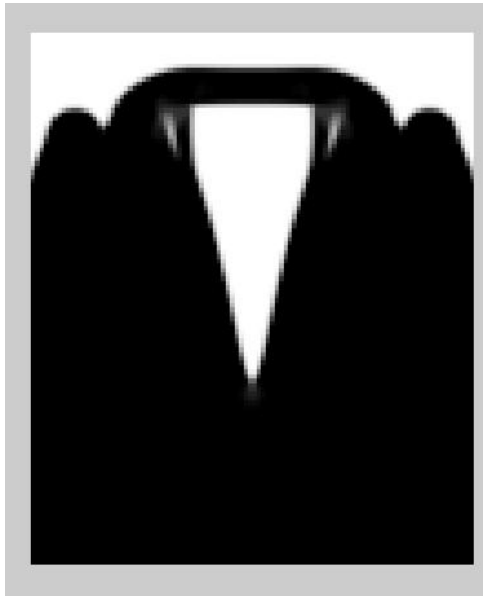
(d) 100,120,0.5,3,1.5  $f=-1000$



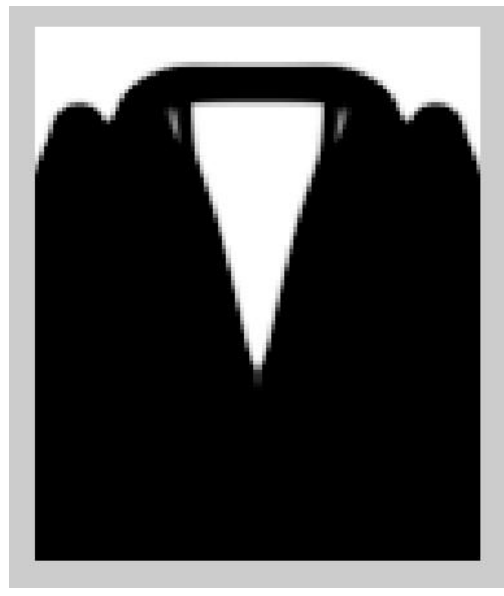
(e)100,120,0.6,3,1.5



(f)100,120,0.7,3,1.5



(g)100,120,0.8,3,1.5 E=10



(h)100,120,0.8,3,1.5 f=-100



(i)100,120,0.8,3,1.5



(j)100,120,0.9,3,1.5

Fig 5.2 Results of simulation, the back part exoskeleton 2-D shapes under different volume rate requirements

In Fig 5.2 we can see the shape change of back part exoskeleton under different volume rate, from 0.5 to 0.9.

In (a), (b), (c), (d), the middle part of the block is totally empty, this is reasonable because there is no force in middle part, it is not necessary to distribute material here.

In (a), (b), we see in (b), the boundary of the shape is not so clear as the shape boundary shown in (a), I assume this is because the filter size of (b) is bigger than (a). Generally the filter size should be larger than 1, as the number of grids increase, the filter size should increase too.

In (a) and (c), the change of penalization power seems does not change the result.

In (a) and (d), we change the forces value from -1 to -1000, there is no clear difference in the results. I think this is because of our model, our model is a 2-D block, we cannot see the change of thickness. If we can do a 3-D shape optimization, the change of thickness can be seen clearly.

In (a), (e), (f), (i) and (j), the difference of results can be seen clearly. As the volume rate increase, the shape of back part exoskeleton becomes to be like a “shirt”. “Collar” is formed at first, then the “collar” is becoming smaller and smaller.

In (g) and (i), we can see the difference due to the change of Young’s modulus  $E$ , for bigger  $E$ , two holes near the collar are bigger.

It tells us the most important part in the model, the second important part, and unimportant part. They are two sides where exerted the forces, the connection part between two sides, and the middle part, respectively. We need to enforce the parts that are important, eliminate unimportant part to make exoskeleton lighter.



## REFERENCE

1. "ErgoAg Company, P.O. Box 1087, Aptos CA. 95001." (n.d.). .
2. Abdoli-E, Mohammad, Michael J. Agnew, and Joan M. Stevenson. "An on-body personal lift augmentation device (PLAD) reduces EMG amplitude of erector spinae during lifting tasks." *Clinical Biomechanics* 21, no. 5 (2006): 456-465.
3. Anderson, Robert B., and R. M. D. (1993). "Stoop labor assist device." U.S.
4. Mitchell and Timothy John. (2002). "Upper body support." U.S.
5. Roberts, B. (1999). "Back-mounted mobile back support device." U.S.
6. Sankai, Y. (2010). "HAL: Hybrid Assistive Limb Based on Cybernetics." *Springer Tracts in Advanced Robotics*, 66(STAR), 25–34.
7. Zoss, A., Kazerooni, H., and Chu, A. (1960). "On the Mechanical Design of the Berkeley Lower Extremity Exoskeleton ( BLEEX )."
8. Martin, Lockheed. "HULC Robotic Exoskeleton." *Lockheed Martin Corp., Bethesda, MD*, <http://www.lockheedmartin.com/us/products/hulc/hulcpress-releases.html> (2011).
9. Lee, Kok-Meng, and Donghai Wang. "Design analysis of a passive weight-support lower-extremity-exoskeleton with compliant knee-joint." In *Robotics and Automation (ICRA), 2015 IEEE International Conference on*, pp. 5572-5577. IEEE, 2015.
10. Costa, Nelson, and Darwin G. Caldwell. "Control of a biomimetic" soft-actuated" 11. 10dof lower body exoskeleton." In *Biomedical Robotics and Biomechatronics, 2006. BioRob 2006. The First IEEE/RAS-EMBS International Conference on*, pp. 495-501. IEEE, 2006.
12. Chen, Chunjie, Duan Zheng, Ansi Peng, Can Wang, and Xinyu Wu. "Flexible design of a wearable lower limb exoskeleton robot." In *Robotics and Biomimetics (ROBIO), 2013 IEEE International Conference on*, pp. 209-214. IEEE, 2013.
13. Asbeck, Alan T., Stefano MM De Rossi, Kenneth G. Holt, and Conor J. Walsh. "A biologically inspired soft exosuit for walking assistance." *The International Journal of Robotics Research* (2015): 0278364914562476.

14. Wehner, Michael, Brendan Quinlivan, Patrick M. Aubin, Ernesto Martinez-Villalpando, Martin Baumann, Leia Stirling, Kenneth Holt, Roger Wood, and Conor Walsh. "A lightweight soft exosuit for gait assistance." In *Robotics and Automation (ICRA), 2013 IEEE International Conference on*, pp. 3362-3369. IEEE, 2013.
15. Kim, Wansoo, Heedon Lee, Donghwan Kim, Jungsoo Han, and Changsoo Han. "Mechanical design of the Hanyang Exoskeleton Assistive Robot (HEXAR)." In *Control, Automation and Systems (ICCAS), 2014 14th International Conference on*, pp. 479-484. IEEE, 2014.
16. Walsh, Conor James, Ken Endo, and Hugh Herr. "A quasi-passive leg exoskeleton for load-carrying augmentation." *International Journal of Humanoid Robotics* 4, no. 03 (2007): 487-506.
17. Krut, Sébastien, Michel Benoit, Etienne Dombre, and François Pierrot. "Moonwalker, a lower limb exoskeleton able to sustain bodyweight using a passive force balancer." In *Robotics and Automation (ICRA), 2010 IEEE International Conference on*, pp. 2215-2220. IEEE, 2010.
18. Huo, Weiguang, Sabah Mohammed, Juan C. Moreno, and Yacine Amirat. "Lower limb wearable robots for assistance and rehabilitation: A state of the art." (2014).
19. Farris, Ryan J., Hugo A. Quintero, and Michael Goldfarb. "Preliminary evaluation of a powered lower limb orthosis to aid walking in paraplegic individuals." *Neural Systems and Rehabilitation Engineering, IEEE Transactions on* 19, no. 6 (2011): 652-659.
20. Cheng, Chi-Hung. "Dynamics and Control of Two Degree-of-Freedom Suspension System with Application to Rehabilitation." (2011).

## APPENDIX

### Code of Shape Optimization of Backside Exoskeleton

```
function top(nelx,nely,volfrac,penal,rmin);
% INITIALIZE
x(1:nely,1:nelx) = volfrac;
loop = 0;
change = 1.;
% START ITERATION
while change > 0.01
    loop = loop + 1;
    xold = x;
% FE-ANALYSIS
    [U]=FE(nelx,nely,x,penal);
% OBJECTIVE FUNCTION AND SENSITIVITY ANALYSIS
    [KE] = lk;
    c = 0.;
    for ely = 1:nely
        for elx = 1:nelx
            n1 = (nely+1)*(elx-1)+ely;
            n2 = (nely+1)* elx +ely;
            Ue = U([2*n1-1;2*n1; 2*n2-1;2*n2; 2*n2+1;2*n2+2; 2*n1+1;2*n1+2],1);
            c = c + x(ely,elx)^penal*Ue'*KE*Ue;
            dc(ely,elx) = -penal*x(ely,elx)^(penal-1)*Ue'*KE*Ue;
        end
    end
% FILTERING OF SENSITIVITIES
    [dc] = check(nelx,nely,rmin,x,dc);
% DESIGN UPDATE BY THE OPTIMALITY CRITERIA METHOD
    [x] = OC(nelx,nely,x,volfrac,dc);
% PRINT RESULTS
    change = max(max(abs(x-xold)));
    disp([' It.: ' sprintf('%4i',loop) ' Obj.: ' sprintf('%10.4f',c) ...
        ' Vol.: ' sprintf('%6.3f',sum(sum(x))/(nelx*nely)) ...
        ' ch.: ' sprintf('%6.3f',change )])
% PLOT DENSITIES
    colormap(gray); imagesc(-x); axis equal; axis tight; axis off;pause(1e-6);
end
%%%%%%%%%%%%%%%%%%%%%%%%%%%%%%%%%%%%%%%%%%%%%%%%%%%%%%%%%%%%%%%%%%%%%%%%% OPTIMALITY CRITERIA
UPDATE %%%%%%%%%%%%%%%%%%%%%%%%%%%%%%%%%%%%%%%%%%%%%%%%%%%%%%%%%%%%%%%%%%%%%%%%%%
function [xnew]=OC(nelx,nely,x,volfrac,dc)
l1 = 0; l2 = 100000; move = 0.2;
while (l2-l1 > 1e-4)
```

```

lmid = 0.5*(l2+l1);
xnew = max(0.001,max(x-move,min(1.,min(x+move,x.*sqrt(-dc./lmid)))));
if sum(sum(xnew)) - volfrac*nelx*nely > 0;
    l1 = lmid;
else
    l2 = lmid;
end
end
end
%%%%%%%%%%%%%%%%%%%%%%%%%%%%%%%%%%%%%%%%%%%%%%%%%%%%%%%%%%%%%%%%%%%%%%%% MESH-INDEPENDENCY
FILTER %%%%%%%%%%%%%%%%%%%%%%%%%%%%%%%%%%%%%%%%%%%%%%%%%%%%%%%%%%%%%%%%%%%%%%%%%
function [dcn]=check(nelx,nely,rmin,x,dc)
dcn=zeros(nely,nelx);
for i = 1:nelx
    for j = 1:nely
        sum=0.0;
        for k = max(i-floor(rmin),1):min(i+floor(rmin),nelx)
            for l = max(j-floor(rmin),1):min(j+floor(rmin),nely)
                fac = rmin-sqrt((i-k)^2+(j-l)^2);
                sum = sum+max(0,fac);
                dcn(j,i) = dcn(j,i) + max(0,fac)*x(l,k)*dc(l,k);
            end
        end
        dcn(j,i) = dcn(j,i)/(x(j,i)*sum);
    end
end
end
%%%%%%%%%%%%%%%%%%%%%%%%%%%%%%%%%%%%%%%%%%%%%%%%%%%%%%%%%%%%%%%%%%%%%%%%
FE-ANALYSIS %%%%%%%%%%%%%%%%%%%%%%%%%%%%%%%%%%%%%%%%%%%%%%%%%%%%%%%%%%%%%%%%%%%%%%%%%
function [U]=FE(nelx,nely,x,penal)
[KE] = lk;
K = sparse(2*(nelx+1)*(nely+1), 2*(nelx+1)*(nely+1));
F = sparse(2*(nely+1)*(nelx+1),1); U = zeros(2*(nely+1)*(nelx+1),1);
for elx = 1:nelx
    for ely = 1:nely
        n1 = (nely+1)*(elx-1)+ely;
        n2 = (nely+1)* elx    +ely;
        edof = [2*n1-1; 2*n1; 2*n2-1; 2*n2; 2*n2+1; 2*n2+2; 2*n1+1; 2*n1+2];
        K(edof,edof) = K(edof,edof) + x(ely,elx)^penal*KE;
    end
end
end
% DEFINE LOADS AND SUPPORTS (HALF MBB-BEAM)
% F(2,1) = -1;
% fixeddofs = union([1:2*(nely+1)],[2*(nelx+1)*(nely+1)]);
F(floor(1*nelx/10)*2*(nely+1)+2*floor(nely/5)+2,1) = -1;
F(floor(2*nelx/10)*2*(nely+1)+2*floor(nely/5)+2,1) = -1;

```

```

F(floor(8*nex/10)*2*(nely+1)+2*floor(nely/5)+2,1) = -1;
F(floor(9*nex/10)*2*(nely+1)+2*floor(nely/5)+2,1) = -1;
% fixeddofs =
union(union([1:2:2*(nely+1)],[2*nely+1:2*(nely+1):2*(nex+1)*(nely+1)-1]),[2*(nely+1):2*(nely+1):2*(nex+1)*(nely+1)]);
fixeddofs =
union([2*nely+1:2*(nely+1):2*(nex+1)*(nely+1)-1],[2*(nely+1):2*(nely+1):2*(nex+1)*(nely+1)]);
alldofs = [1:2*(nely+1)*(nex+1)];
freedofs = setdiff(alldofs,fixeddofs);
% SOLVING
U(freedofs,:) = K(freedofs,freedofs) \ F(freedofs,:);
U(fixeddofs,:)= 0;
%%%%%%%%%% ELEMENT STIFFNESS
MATRIX %%%%%%%%%%%
function [KE]=lk
E = 1.;
nu = 0.3;
k=[ 1/2-nu/6    1/8+nu/8 -1/4-nu/12 -1/8+3*nu/8 ...
    -1/4+nu/12 -1/8-nu/8    nu/6      1/8-3*nu/8];
KE = E/(1-nu^2)*[ k(1) k(2) k(3) k(4) k(5) k(6) k(7) k(8)
                  k(2) k(1) k(8) k(7) k(6) k(5) k(4) k(3)
                  k(3) k(8) k(1) k(6) k(7) k(4) k(5) k(2)
                  k(4) k(7) k(6) k(1) k(8) k(3) k(2) k(5)
                  k(5) k(6) k(7) k(8) k(1) k(2) k(3) k(4)
                  k(6) k(5) k(4) k(3) k(2) k(1) k(8) k(7)
                  k(7) k(4) k(5) k(2) k(3) k(8) k(1) k(6)
                  k(8) k(3) k(2) k(5) k(4) k(7) k(6) k(1)];

```

## **VITA**

The author was born in Henan Province, China on January 1<sup>st</sup>, 1992. He was awarded Bachelor of Engineering degree in Mechanical Engineering from Zhejiang University, Hangzhou, China, in June, 2014. Then he attended Lehigh University pursuing a Master of Science degree supervised by Professor Meng-Sang Chew. The author was especially interested in the research of robotics, exoskeleton and control.